2022

Ferrihydrite enrichment in the rhizosphere of unsaturated soil improves nutrient retention while limiting arsenic and uranium plant uptake

Arindam Malakar

Daniel D. Snow

Michael Kaiser

Jordan Shields

Bijesh Maharjan

See next page for additional authors

Authors

Arindam Malakar, Daniel D. Snow, Michael Kaiser, Jordan Shields, Bijesh Maharjan, Harkamal Walia, Daran Rudnick, and Chittaranjan Ray

Ferrihydrite enrichment in the rhizosphere of unsaturated soil improves nutrient retention while limiting arsenic and uranium plant uptake

Arindam Malakar,[1] Daniel D. Snow,[2] Michael Kaiser,[3] Jordan Shields,[4] Bijesh Maharjan,[5] Harkamal Walia,[3] Daran Rudnick,[6] and Chittaranjan Ray [7]

1 Nebraska Water Center, part of the Robert B. Daugherty Water for Food Global Institute, Water Sciences Laboratory, University of Nebraska, Lincoln, NE 68583-0844, United States; *email* amalakar2@unl.edu

2 Nebraska Water Center, part of the Robert B. Daugherty Water for Food Global Institute, Water Sciences Laboratory, School of Natural Resources, University of Nebraska, Lincoln, NE 68583-0844, United States

3 Department of Agronomy and Horticulture, University of Nebraska-Lincoln, Lincoln, NE 68583-0915, United States

4 School of Natural Resources, Nebraska Water Center, part of the Robert B. Daugherty Water for Food Global Institute, Water Sciences Laboratory, University of Nebraska, Lincoln, NE 68583-0844, United States

5 Department of Agronomy and Horticulture, University of Nebraska-Lincoln, Panhandle Research and Extension Center, 4502 AVE I, Scottsbluff, NE 69361-4939, United States

6 Biological Systems Engineering Department, 247 L.W. Chase Hall, University of Nebraska-Lincoln, Lincoln, NE 68583-0726, United States

7 Nebraska Water Center, part of the Robert B. Daugherty Water for Food Global Institute 2021 Transformation Drive, University of Nebraska, Lincoln, NE 68588-6204, United States

Corresponding author — C. Ray, cray@nebraska.edu

Published in *Science of the Total Environment* 806 (2022) 150967
doi:10.1016/j.scitotenv.2021.150967

Submitted 27 August 2021; revised 3 October 2021; accepted 9 October 2021; published 14 October 2021.

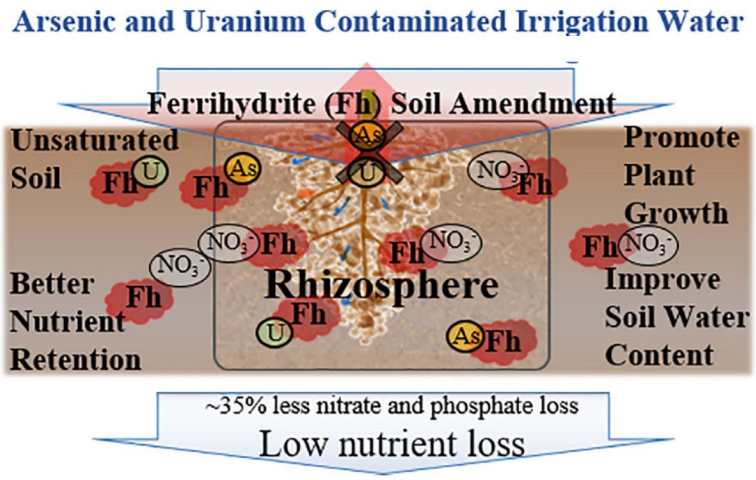

Abstract

Improvement of nutrient use efficiency and limiting trace elements such as arsenic and uranium bioavailability is critical for sustainable agriculture and food safety. Arsenic and uranium possess different properties and mobility in soils, which complicates the effort to reduce their uptake by plants. Here, we postulate that unsaturated soil amended with ferrihydrite nanominerals leads to improved nutrient retention and helps reduce uptake of these geogenic contaminants. Unsaturated soil is primarily oxic and can provide a stable environment for ferrihydrite nanominerals. To demonstrate the utility of ferrihydrite soil amendment, maize was grown in an unsaturated agricultural soil that is known to contain geogenic arsenic and uranium. The soil was maintained at a gravimetric moisture content of 15.1 ± 2.5%, typical of periodically irrigated soils of the US Corn Belt. Synthetic 2-line ferrihydrite was used in low doses as a soil amendment at three levels (0.00% w/w (control), 0.05% w/w and 0.10% w/w). Further, the irrigation water was fortified (~50 μg L^{-1} each) with elevated arsenic and uranium levels. Plant dry biomass at maturity was ~13.5% higher than that grown in soil not receiving ferrihydrite, indicating positive impact of ferrihydrite on plant growth. Arsenic and uranium concentrations in maize crops (root, shoot and grain combined) were ~ 20% lower in amended soils than that in control soils. Our findings suggest that the addition of low doses of iron nanomineral soil amendment can positively influence rhizosphere geochemical processes, enhancing nutrient plant availability and reduce trace contaminants plant uptake in sprinkler irrigated agroecosystem, which is 55% of total irrigated area in the United States.

Keywords

Nanotechnology, Soil amendment, Agricultural soil, Nutrient retention, Plant biomass

Highlights

- Improved nutrient use and reduced trace element uptake is critical in agroecosystem.
- Naturally occurring nanominerals of iron can influence nutrient and trace element.
- Ferrihydrite, a natural iron nanomineral, was produced and used as soil amendment.
- Low doses of amendment improved nutrient retention and reduced trace element uptake.
- Nanotechnology-based amendments of natural nanominerals can improve plant growth.

1. Introduction

Ferrihydrite (Fh), a ubiquitous iron (III) oxyhydroxide nanomineral, occurring naturally in soil, surfacewater, and groundwater (Cornell and Schwertmann, 2003; Tong et al., 2020). Fh's nanosize provides high surface area, which can sequester significant quantities of trace elements (Cornell, 1988; Jambor and Dutrizac, 1998; Vu et al., 2010), but Fh transformation can release sequestered elements (Cornell and Schwertmann, 2003). The transformation rate is controlled by pH (Das et al., 2011a; Schwertmann, 1983; Shaw, 2005), temperature (Das et al., 2011a), ionic strength (Cornell, 1988; Das et al., 2011b; Jang et al., 2003), and organic matter (Hu et al., 2018; Zhou et al., 2018). Fh transformation can occur within days under anoxic conditions (Perez et al., 2019). At near-neutral pH, under oxic conditions, it is slow, taking weeks, months to years to show any mineralogical changes (Perez et al., 2019; Schwertmann et al., 2004; Zhang et al., 2019). Fh is relatively stable in oxic conditions prevalent in non-flooded irrigated agricultural soils (Wagner, 2017), which comprises 55% of the US's total irrigated area (Dieter et al., 2018). Thus, under unsaturated conditions prevalent in the sprinkler, drip, or furrow irrigation, Fh transformation will occur slowly and may be limited to anoxic microsites (Hall and Silver, 2015; Han et al., 2019; Malakar et al., 2020; Yang et al., 2012) of the unsaturated zone. Fh is expected to persist for prolonged periods in unsaturated soil, and its use as soil amendment may provide improved nutrient retention and limit trace element mobilization.

The topsoil in large areas of the US Corn Belt contains significant quantities of naturally-occurring arsenic (As) and uranium (U) (Smith et al., 2011, 2013a). Plants grown in soil with elevated concentrations

of these trace elements may be prone to bioaccumulation, which may impact human health (Boghi et al., 2018; Bundschuh et al., 2012; Heikens et al., 2007; Malakar et al., 2019; Shi et al., 2020; Wang et al., 2017). Therefore, it is necessary to understand their bioavailability in unsaturated agricultural soils and devise plans to mitigate their occurrence in agricultural products. Arsenic can be present as arsenite or arsenate (As(III/V)) oxyanion (Malakar et al., 2016a), and mobilization is sensitive to the redox conditions and pH of soil or water. The reduced form of arsenic is more mobile, whereas for uranium, oxidized cation (uranyl ion: $U(VI)O_2^{2+}$) is mobile, and U(IV), the reduced form, is considered to be immobile (Malakar et al., 2016a; Vodyanitskii, 2011). In unsaturated soil, the oxidized forms of arsenic and uranium are more prevalent, and various biogeochemical processes of unsaturated soils can influence the bioavailability of these contaminants (Boghi et al., 2018; Hall and Silver, 2015; Han et al., 2019; Malakar et al., 2020; Yang et al., 2012). Interactions with iron oxides/hydroxides affect many trace contaminants and nutrients mobility and bioavailability (Dietrich et al., 2016; Malakar et al., 2016b, 2020; Sherman and Randall, 2003; Sparks, 2003; Vodyanitskii, 2011; Vodyanitskii and Shoba, 2016; Wedepohl, 1991). Iron is an essential nutrient for crops, and uptake by reduction or chelation can influence iron geochemistry in the soil (Colombo et al., 2014; Keiluweit et al., 2017; Malakar et al., 2020; Yang et al., 2012). Fh plays a critical role within rhizosphere processes of unsaturated soil (Hall and Silver, 2015; Han et al., 2019; Malakar et al., 2020; Yang et al., 2012) and elevated Fh levels as soil amendment at the root zone-soil-porewater interface can change distribution and mobility of nutrients and trace elements. Understanding this relationship is the primary focus of the present work.

Here, we show that adding Fh to the rhizosphere of unsaturated agricultural soil can limit arsenic and uranium bioavailability and enhance soil nutrient retention. Fh's essential role is established through increased plant biomass, improved nutrient availability and decrease in trace element plant uptake. Using a greenhouse experimental system, we simulated the soil water content similar to unsaturated conditions typical of periodically irrigated soils of the US Corn Belt (Bowman et al., 1991). Anoxic microsites at the root zone-soil-porewater interface of unsaturated soils are hotspots for coupled iron/nutrient-contaminant cycles (Hall and Silver, 2015; Han et al., 2019; Malakar et al., 2020; Yang

et al., 2012). Therefore, identifying the effect of Fh enrichment on geochemical pathways in the rhizosphere is critical to improve sustainable soil productivity and limit the mobility of trace elements.

2. Materials and methods

2.1. Materials

Reagents, including iron (III) chloride ($FeCl_3$) reagent grade (97%), sodium bicarbonate (ACS reagent, >99.7%, $NaHCO_3$), trisodium citrate dihydrate (ACS reagent, ≥99%), ferrous sulfate (99.9%), ammonium acetate (99.9%), acetic acid (99.9%), calcium carbonate (ACS reagent, ≥99%), sodium nitrite (ReagentPlus®, ≥99.0%), and 1,10-phenanthroline (99.9%) were purchased from Sigma-Aldrich, USA. Sulfanilamide (Certified ACS, Fisher Chemical), N-(1-Naphthyl)ethylenediamine, dihydrochloride (98+%, ACS reagent), zinc acetate dihydrate ($Zn(CH_3COO)_2.2H_2O$) (extra pure, 98%), ammonium carbonate (ACS reagent, $(NH_4)_2CO_3$), sodium hydrosulfite (ca. 85%, Tech., $Na_2S_2O_4$), and potassium hydroxide (KOH) were manufactured by ACROS organics™ and purchased from Fisher Scientific, USA. Arsenic and uranium standards were purchased from Inorganic™ Venture, USA. Arsenite (As(III)) and Arsenate (As(V)) reference standards were purchased from Millipore Sigma, USA. All water used in the experiment was reagent grade with a resistivity of 18.2 MΩ-cm.

2.2. Synthesis of 2-line ferrihydrite

Synthetic 2-line ferrihydrite (Fh) was prepared following method described elsewhere (Islam et al., 2020; Malakar et al., 2020). Briefly, Fh was prepared by dissolving 25 g of $FeCl_3$ salt in 10 L of reagent grade water. The pH of this solution mixture was brought to near neutral by controlled addition of 1 M KOH, and pH was kept around 6.5 ± 0.2. Finally, 0.15 g of $Zn(CH_3COO)_2.2H_2O$ was added and mixed well to precipitate the 2-line Fh. The solution was decanted to reduce the volume and filtered (Whatman 42, GE Healthcare, USA). The precipitate was dried in a vacuum desiccator for 48 h before use. Powder x-ray diffraction (PXRD) (PANalytical Empyrean Diffractometer, Cu K_α source) was carried out to

confirm the formation of 2-line Fh, which matched well to the (110) and (115) planes (Fig. S1) of 2-line Fh (PCPDF# 29-0712) (Islam et al., 2020; Malakar et al., 2020; Zhu et al., 2015).

2.3. Greenhouse experiment

The experiment design was modified from Malakar et al. (2020). The soil used in the experiment was collected on April 2019 from a field site located at the University of Nebraska-Lincoln (UNL) Panhandle Research, Extension, and Education Center, Scottsbluff, Nebraska (41° 53' 36.22466", –103° 40' 51.30451"). The soil classified as Tripp is a very fine sandy loam soil (coarse-silty, mixed, superactive, mesic Aridic Haplustolls) (Elder, 1969) and was collected within a 10 m by 10 m by 10 cm (depth) grid. The field had been planted to maize in the previous growing season. The average precipitation at Scottsbluff is 401 mm and average snowfall is 109.2 cm, in summer the average high temperature is 33.4 °C and in winter average low temperature is –9.9 °C. The soil was air-dried in a greenhouse and sieved through 2 mm mesh, before the start of the experiment. Air-dried soil pH was 7.5±0.1 and soil organic matter content was 18 ± 2 g kg^{-1}. The residual nitrate and ammonia concentrations of the air-dried soil were at 2.3 ± 0.6 μg-N g^{-1}, and 0.7 ± 0.2 μg-N g^{-1}, respectively. Agricultural soil contained arsenic (2.9 ± 0.4 μg g^{-1}), and uranium (1.1 ± 0.2 μg g^{-1}), which are of geogenic origin (Smith et al., 2013b).

Eight kilograms of air-dried soil were weighed out in each polyethylene planting pots (n = 18) of 25 cm diameter. The eighteen pots were divided into three groups. One set of six received no Fh (Control = 0.00% w/w, n = 6). Another set of six received 0.05% w/w Fh, (n = 6), and the final set received 0.10% w/w Fh (n = 6) as a soil amendment. Fh was applied by dispersal in 50 g of reagent grade water and mixed in the top 5 cm of the soil layer. The top 5 cm soils of control pots were mixed only with 50 g of reagent grade water. Three maize seeds (cultivar-Dekalb®, DKC46-36RIB Brand Blend) were added to each pot, and thinned to one plant after germination. Maize was grown for 105 days and had formed grains (kernels) by the end of the experiment. The temperature was maintained between 22 and 28 °C. The crops received 16 h of daily light, the maximum level for summer growing season. Irrigation water (pH = 6.9 ± 0.1) was fortified with arsenic and uranium

from standard solutions (Inorganic™Venture, USA) in distilled water. The elevated concentrations of arsenic and uranium in irrigation water were used to examine the potential effect of Fh on plant uptake. A modified Hoagland solution (Hoagland and Arnon, 1950) was used to supply macro and micro-nutrients required for crop growth and limit crop stress. Since iron was provided as Fh amendment, the Hoagland solution was devoid of iron (Malakar et al., 2020). No phosphorous was added as phosphorous fertilizer is not generally used for crop production in these soil types. Phosphate is also known to bind strongly to Fh (Wang et al., 2013), and Fh can potentially limit phosphate bioavailability (Rhoton and Bigham, 2005). The modified Hoagland solution was prepared without phosphate to evaluate the impact of Fh addition on crop phosphate availability as provided from the soil. Modified Hoagland solution (250 g) was applied on day 7, and 100 g was applied on day 31 and 61 following porewater collection.

An equal amount (200 g) of irrigation water was applied to each pot every other week from day 21. Soil water content in the top 15 cm, near the crop, was measured twice a week using a handheld moisture probe (Extech MO750 Soil Moisture Meter, FLIR Commercial Systems Inc., Nashua, NH, USA) (Deng et al., 2015) and gravimetrically every other week. Porewater from each pot was collected as leachate in a clean tray placed at the bottom of pots on Days 30, 60, and 90 of sowing seeds. Equal quantities (1500 g) of irrigation water were uniformly applied in each pot, and within 30 min, porewater samples were collected in a tray. After day 31, irrigation water was not applied as unsaturated conditions were maintained (Fig. S2). Plant stress was monitored by measuring chlorophyll content bi-weekly using a chlorophyll meter (SPAD-502, Minolta, Tokyo, Japan) averaging five readings of the tallest fully collared leaf (Zhang et al., 2009). Plant height was measured biweekly from the soil surface to the arch of the uppermost leaf (Freeman et al., 2007).

2.4. Porewater, soil, and plant tissue analyses

Collected porewater samples were filtered using 0.45 μm syringe filter and sub-sampled. Given the size range of added Fh (Michel et al., 2007) and organic-iron complexes (Ritter et al., 2006) formed in the rhizosphere, chances of including colloidal iron in filtered porewater are high but may be considered to be part of the dissolved iron phase (Ritter et

al., 2006). Porewater samples were analyzed in situ within 10 min of collection for reduced iron (Fe^{2+}), and nitrite spectrophotometrically (Kaifer, 1992; Oliveira et al., 2006; Tamura et al., 1974; Zhu et al., 2018). Within 48 h, unpreserved sub-samples were used to measure alkalinity, dissolved organic carbon (DOC), major anions (fluoride, chloride, bromide, phosphate and sulfate) and inorganic arsenic species (Kutscher et al., 2012; Yu et al., 2019). Subsamples for nitrate, and ammonium were preserved with sulfuric acid, whereas hydrochloric acid was used to preserve arsenic, uranium, total iron, major cations subsamples. Porewater arsenic and uranium concentration reported here has been deducted from the concentration present in irrigation water, which were 48.8 ± 2.0 μg L^{-1} and 49.8 ± 0.9 μg L^{-1} for arsenic and uranium, respectively.

Soil pH (Oakton PHTestrs 30), by 1:1 soil:water solution, and oxidation-reduction potential (ORP) (Oakton ORPTestr 50), at 5 cm depth, were measured bi-weekly. Soil samples from each pot were collected at Day 0, midpoint (Day 45), and endpoint (Day 105). Air-dried soil samples were analyzed for dithionite-citrate-bicarbonate (DCB) extractable iron (Colombo et al., 2014), acid-leachable iron, arsenic, and uranium by inductively coupled plasma mass spectrometry (Thermo Dionex IC 5000+ iCAP RQ, ICP MS). Mid (Day 45) and endpoint (Day 105) soils with visible roots were collected as root zone or rhizosphere soil samples, and soil near the edge of the pot with no visible roots was collected as bulk soil samples. Acid-leachable arsenic and uranium quantification were carried out after microwave digestion of the air-dried soil samples (Link et al., 1998; United States Environmental Protection Agency (EPA), 1996). DCB extraction was carried out for quantifying extractable iron in the soil (Amaral et al., 2017; Malakar et al., 2020). All digests and extracts were analyzed without further dilution using ICP-MS and for iron after 100-fold dilution, with matrix match standards. Soil certified reference materials (CRMs) were processed using identical methods to check accuracy for elemental measurements.

The first group of plant samples (n=3)were harvested at midpoint (Day 45), and the final harvest (n=3)was at endpoint (Day 105). Crop samples were washed with reagent grade water and dried in an oven at 65 °C to constant weight. Plant dry biomass weight was recorded, roots shoots and grains/kernels (wherever available) were separated and quantified by ICP-MS. The dried samples were weighed and ground to pass through a 100-mesh sieve for elemental analysis with ICP-MS

(United States Environmental Protection Agency (EPA), 1996). Dry weight plant concentrations of trace elements have been reported in this study. The bioaccumulation factor (BF) of trace elements in plants and the transfer factors (TFs) from root to shoot and shoot to kernel, were calculated to determine the degree of metal accumulation in the plants (Yashim et al., 2014), following equation,

$$BF = \frac{\text{Concentration of trace elements in plants}}{\text{Concentration of trace elements in soil}}$$

$$TF = \frac{\text{Concentration of trace elements in plant shoot or kernel}}{\text{Concentration of trace elements in plant root or shoot}}$$

Detailed porewater, soil and plant tissue analysis methods are available in the supplementary data.

2.5. Statistical analyses

Statistical analysis was carried out in Origin Pro, Version 2020b (OriginLab Corporation, USA). Data shown here in figures and tables of the article and supplementary data is presented as mean ± standard deviation, error bars in figures are standard deviation. Data were tested for normal distribution and homogeneity of variance. Pearson correlation coefficients and one-way ANOVA analysis with post hoc Tukey test were performed to statistically analyze significant effects of the factor soil Fh amendment (0.00%, 0.05%, and 0.10% Fh) on selected parameters.

2.6. Chemical equilibrium modeling

The equilibrium model was carried out by adopting the USGS chemical thermodynamics program PHREEQC (version 3) (Parkhurst and Appelo, 2013). The computer program PHREEQC is designed in C language platform and is capable to simulate low-temperature geochemical calculations. The chemical equilibrium is achieved by an ion-association aqueous model and can predict speciation and saturation-indices, which can be implemented in wide variety of reversible and irreversible reactions, which include aqueous, mineral, gas and solid-solution reactions. However, the model is based upon Debye-Hückel expressions

to account for the non-ideality of aqueous solutions, which is adequate at low ionic strength but may break down at higher ionic strengths (in the range of seawater and above) (Parkhurst and Appelo, 2013). With PHREEQC, species, reactions, and equilibrium constants are all defined in a "database" file. The database wateq4f.dat, derived from WATEQ4F (Ball and Nordstrom, 1991) was adopted to calculate the different species of the elements analyzed. This database includes relevant uranium, arsenic, and iron species. The model utilized nitrate/ammonium couple to calculate redox-sensitive species (Kölling, 2000; Nordstrom et al., 1979) and predicted equilibrium concentration of reduced iron and arsenic species in the porewater. The model-predicted values of reduced iron and As (V) were compared with experimental results to validate the model (Malakar et al., 2020). Model inputs included measured temperature, pH, porewater alkalinity, major anions (fluoride, chloride, bromide, sulfate and phosphate), major cations (sodium, potassium, calcium and magnesium), ammonia, total iron, arsenic and uranium concentration in collected porewater (Malakar et al., 2020; Nordstrom et al., 1979).

3. Results and discussion

3.1. Iron redox cycles, trace contaminant mobility, and soil nutrient retention

The irrigation schedule was similar to a typical crop production schedule in the US Midwest (Bowman et al., 1991; Irmak et al., 2000). The gravimetric water content was maintained at 15.1 ± 2.5% (Fig. S2) in all three soil Fh-systems (i.e. 0.00% Fh, 0.05% Fh, 0.10% Fh). In the untreated air-dried soil, DCB extractable iron was 614 ± 56 μg g^{-1}, acid-leachable iron was 9980 ± 588 μg g^{-1}, arsenic was 2.9 ± 0.4 μg g^{-1}, and uranium was 1.1 ± 0.2 μg g^{-1}. From Day 0 to 105, the soil pH was 7.4 ± 0.4, and E_h ORP of bulk soil measured at ~5 cm depth varied from 0.38 to 0.47 V, consistent with suboxic to oxic conditions in the bulk soil (Borch et al., 2010). Development of localized anoxic microsites within the rhizosphere is a gradual process and depends on the sufficient root and plant growth (Malakar et al., 2020), so sufficient periods was given before porewater sampling (i.e., 30- 90 days).

Porewater sampled from all three Fh systems contained reduced iron (Fe^{2+}) (**Fig. 1**a). Cumulative Fe^{2+} concentration (sum of the average concentrations measured at Day 30 (n = 6), and at Days 60 and 90 (n = 3)) was 588.4 μg l^{-1} for 0.00% Fh, 514.2 μg l^{-1} for 0.05% Fh, and 253.0 μg l^{-1} for 0.10%. The Fe^{2+} concentrations were similar in all three Fh-systems at the first sampling point. Porewater Fe^{2+} was highest at Day 60 and decreased back at Day 90, suggesting dynamic iron redox cycles within the growing period of maize. Though the trend of Fe^{2+} concentration was similar in all three Fh-systems, the Fe^{2+} concentration at Day 60 significantly ($p < 0.01$) differed between these systems. The prevalence of Fe^{2+} in the porewater was unexpected, as maize primarily takes up iron by chelation but Fe^{2+} has been observed in previous studies (Malakar et al., 2020; Morrissey et al., 2009). Variations in reduced iron in porewater seemed to influence variations in trace element concentration. Cumulative arsenic concentration was 87.0 μg l^{-1} (0.00% Fh), 71.4 μg l^{-1} (0.05% Fh), and 30.4 μg l- 1 (0.10% Fh). For respective cumulative uranium concentrations, we observed 64.3 μg l^{-1} (0.00% Fh), 50.6 μg l^{-1} (0.05% Fh), and 42.2 μg l^{-1} (0.10% Fh). For all systems through all sampling days, the Fe^{2+} in porewater correlated significantly with arsenic (r = 0.87, $p < 0.01$). The oxidized arsenic species, arsenate, concentration in porewater (Table S1) followed a pattern opposite to Fe^{2+}. The co-occurrence of reduced iron and arsenic species suggests iron reduction controls arsenic mobilization in porewater.

Thermodynamic modeling of the porewater indicated divergent geochemical processes for arsenic and uranium at the root zone-soil-porewater interface. The model predicted reduced iron and arsenate concentrations were similar to experimental values (Tables S1, S2). The model suggests U(VI) as the primary form of uranium at Day 30. In contrast, calcium bound U(VI) carbonate complex and reduced U (IV) species are thermodynamically favored as the experiment progressed. The primary species of arsenic predicted by the model was $HAsO_4^{2-}$, which may be bound to added Fh. The model predicted a higher saturation index of Fh in amended soils, indicating Fh's occurrence in the porewater, which is expected due to the nanosize. At Day 60, Fh's saturation index decreased in all three systems and became negative in 0.00% and 0.05% Fh systems. Fh's saturation index increased at Day 90, and values became positive in 0.00% and 0.05% Fh systems. Variation in Fh saturation index suggest that both dissolution and formation of Fh nanomineral occurs even under unsaturated conditions (Malakar et al., 2020).

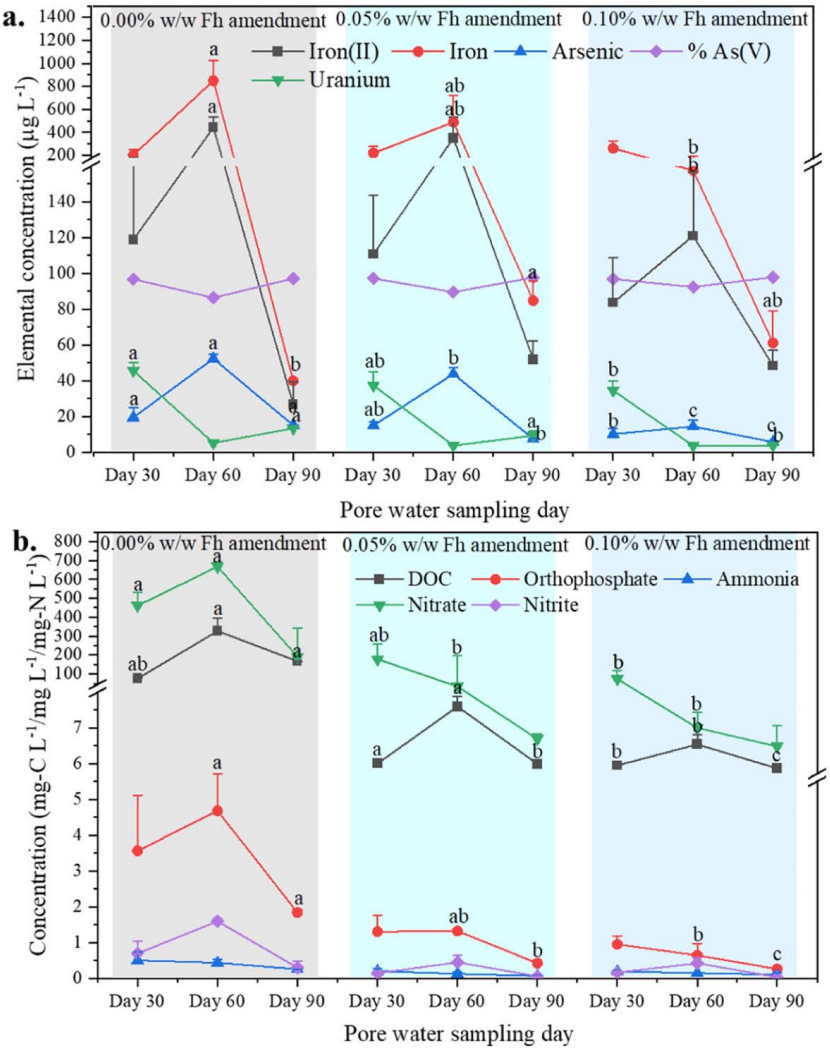

Fig. 1. Changes in concentration of a. reduced iron (iron (II); Fe^{2+}), total iron, arsenic, percentage (%) of arsenate (oxidized form of arsenic), and uranium and b. concentration of dissolved organic carbon (DOC), orthophosphate, ammonia, nitrite and nitrate in the soil porewater after 30, 60 and 90 days of sowing seeds. The Y-axis has a break to show the entire dataset. At Day 60, localized reducing conditions were prevalent as observed from lower percentage of arsenate and higher concentration of iron (II). Increasing DOC likely influences soil redox processes and nutrient mobility. a, b and c on top of data points shows significantly different concentration at $p < 0.01$ as per post hoc Tukey test.

The observed and model-predicted porewater elemental concentration indicates the critical role of elevated Fh-levels in the soil. The availability of hydroxyl surfaces from added Fh can potentially bind Fe^{2+} (Appelo et al., 2002), and decrease Fe^{2+} concentrations in porewater of Fh-enriched systems. The presence of elevated Fh can impact trace contaminant mobility (Malakar et al., 2020), and potentially lowers trace element concentration in porewater of Fh-enriched soils. Dissolution of iron containing mineral or release of adsorbed Fe^{2+} may also contribute to porewater Fe^{2+}(Van Groeningen et al., 2020). Release of bound Fe^{2+} and iron is plausible, as form of arsenic observed in porewater samples is primarily oxidized, which was well supported by the model. The model also predicted oxidized uranium in porewater, as primary format the initial stage of the experiment, indicating iron (or reduced iron) may be coming from dissolution processes (Van Groeningen et al., 2020). However, the rise in Fe^{2+} and reduced arsenic concentration at Day 60 and the subsequent decrease at Day 90 suggest there can be active redox processes in the anoxic microsites of unsaturated soil (Hall and Silver, 2015; Han et al., 2019; Malakar et al., 2020; Yang et al., 2012). The formation of anoxic microsites is also evident from the pattern of observed porewater uranium concentration and model-predicted species. Porewater uranium was highest at Day 30 measurement, as uranium is most mobile in its oxidized form. In contrast to arsenic, lower porewater uranium concentrations occurred at the later stage and may reflect the conversion of highly soluble U(VI) to sparingly soluble U(IV) within the localized redox sites. Along with localized anoxic microsites, release of dissolved Fe^{2+} (Van Groeningen et al., 2020) can explain occurrence of reduced species of iron and arsenic in three Fh-systems irrespective of iron uptake mechanism of maize (Hall and Silver, 2015; Han et al., 2019; Malakar et al., 2020; Yang et al., 2012).

Root exudates, organic acids released by growing roots, are utilized to fulfill crop nutrient demand and also result in increased porewater DOC (Gmach et al., 2020). Root exudate-mediated mineral dissolution processes might also affect the mobility of trace elements in the rhizosphere. In all systems, maximum DOC concentrations were found at Day 60 measurement, pointing towards the influence of exudates from growing roots on porewater DOC (Fig. 1b). Furthermore, porewater DOC in the control was significantly ($p < 0.01$) higher compared to Fh-enriched soils. Fh enrichment resulted in reduced porewater DOC, most likely due

to increased adsorption of dissolved organic moieties on Fh surfaces (Han et al., 2019). Strong positive correlations between overall porewater DOC and overall porewater nitrite ($r = 0.67$, $p < 0.01$), arsenic ($r = 0.85$, $p < 0.01$), arsenite ($r = 0.73$, $p < 0.01$), and Fe^{2+} ($r = 0.67$, $p < 0.01$), and a negative correlation with uranium ($r = -0.62$, $p < 0.01$) across all treatments and sampling dates, suggests tightly coupled redox cycles in the rhizosphere. The release of DOC from roots can also influence microbial redox processes (Coward et al., 2018). Along with transiently saturated soil conditions, DOC release, can support development of localized anoxic microsites in unsaturated soil.

Dissolved ammonia, nitrate, nitrite, and orthophosphate concentrations in porewater at three sampling events are presented in Fig. 1b. Nitrate concentrations differed between the Fh-systems measured on Day 30 and Day 60, with significantly ($p < 0.01$) lower nitrate loss via porewater in the Fh-enriched systems. The lower nitrate loss (~30% for 0.05% Fh and ~48% for 0.10% Fh) in Fh-enriched soils can promote better nitrate utilization, otherwise prone to leaching, and is readily transported with porewater (Green et al., 2008). Like nitrate, porewater orthophosphate (significant, $p < 0.01$), nitrite, and ammonia were lower in Fh-enriched systems. These results indicate that Fh-enriched soils will have better nutrient retention, which may promote plant growth.

3.2. Influence on crop health and trace contaminant uptake

Retention of nutrients in Fh-enriched soils resulted in better plant growth, as observed from dry biomass at two harvesting events, Day 45 (midpoint) and 105 (endpoint) (**Fig. 2**a). Fh-enriched systems had significantly ($p < 0.01$) higher biomass, ~27% higher for 0.05% Fh and ~40% higher for 0.10% Fh at midpoint, and ~ 12% (0.05% Fh) and ~15% (0.10% Fh) higher at endpoint compared to control. Improved plant growth is also indicated in the other plant health indices, including plant relative chlorophyll content and plant height, which were higher in crops from Fh-enriched soils than control (Fig. S3). Fh enrichment provided conditions for better root growth than control and plants did not present signs of iron toxicity (Fig. S4). Iron deficiency (Mariotti et al., 1996; O'Rourke et al., 2007) was not observed in control plants (Fig. S4). Improved crop health indices reveal that nutrients retained in Fh-enriched soils are accessible to the plants.

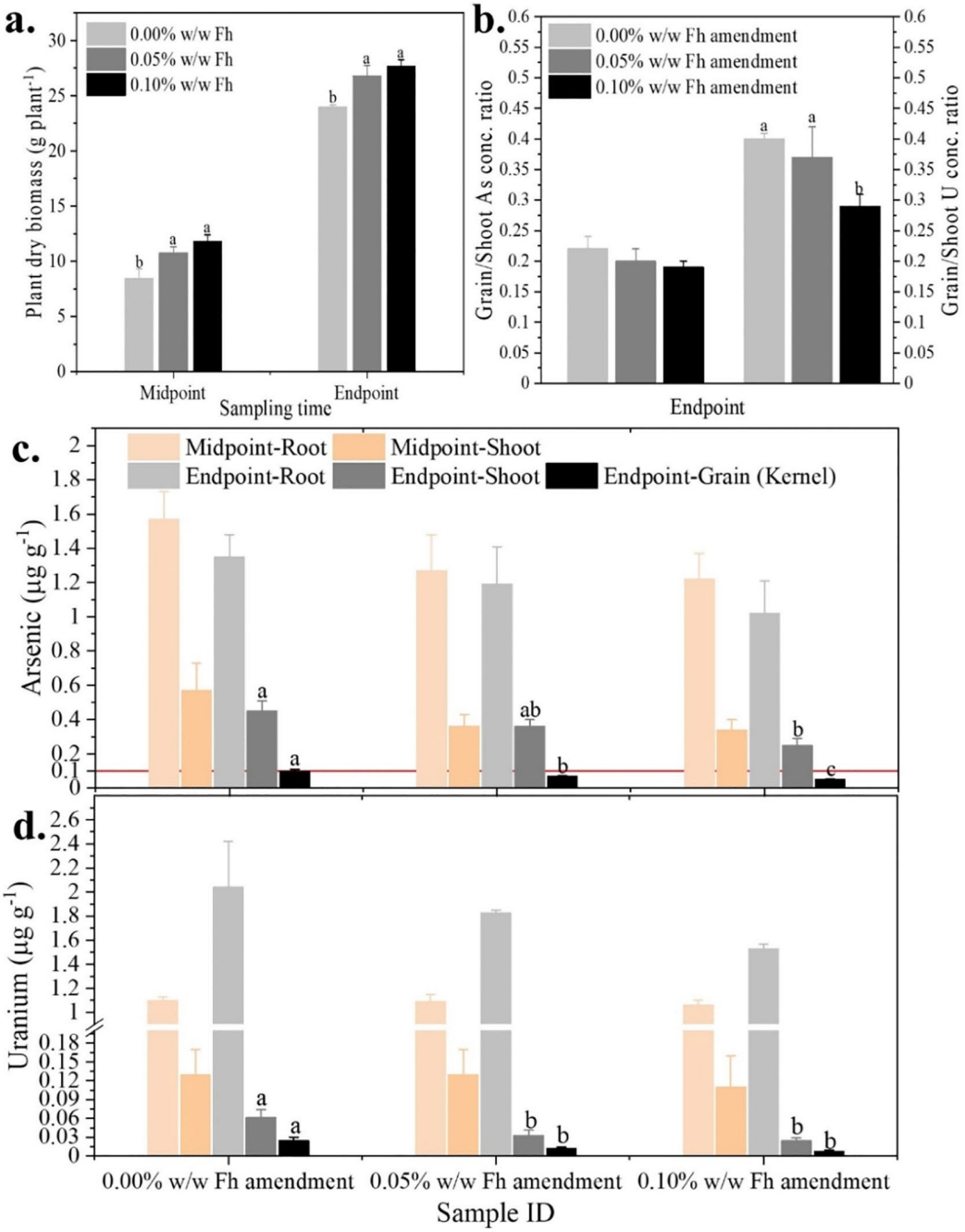

Fig. 2. Crops a. dry biomass, b. grain to shoot arsenic and uranium concentration within the crops, c. arsenic (red line is FDA recommended arsenic level in food grain), and d. uranium concentration in root, shoot and grain (wherever available) in the crops harvested at the mid (Day 45) and endpoint (Day 105) of the experiment. The Y-axis of 2d has a break to show the entire dataset. There is a clear effect of Fh enrichment in the soil, which lowers arsenic and uranium translocation from shoot to root and minimizes uptake of these contaminants within the different parts of the crop. a and b show significantly different concentration at $p < 0.01$ as per post hoc Tukey test. Bars without letter means interactions were not significant.

Interference to phosphorus plant availability from Fh addition has been previously reported (Gypser et al., 2018). In contrast, the plants from Fh-enriched soils in this study presented comparable phosphorus content as in control. At midpoint, phosphorus was 2050 ± 225 μg g^{-1} for 0.10% Fh, 2075 ± 423 μg g^{-1} for 0.05% Fh, and 2104 ± 108 μg g^{-1} for 0.00% Fh. At endpoint, phosphorus content in Fh-enriched soils were 2219 ± 767 μg g^{-1} for 0.10% Fh, 2144 ± 221 μg g^{-1} for 0.05% Fh, and 2253 ± 835 μg g^{-1} for 0.00% Fh, and the differences were insignificant. The mature grains/kernels also had similar phosphorus in Fh-enriched systems (3127 ± 186 μg g^{-1} for 0.10% Fh and 3047 ± 497 μg g^{-1} for 0.05% Fh) and control (3099±828 μg g^{-1}). The concentration of phosphorus in the present study was comparable to field studies, where phosphorus was not supplied externally (Gagnon et al., 2020). The average grain phosphorus concentration in three-year study was found to be 2933±153 μg g^{-1} (Gagnon et al., 2020). Further, in the present study phosphorus was lost during the porewater collection, and was not externally replenished, which may be the reason of lower phosphorus at the midpoint plant samples. However, the phosphorus values of the midpoint maize plant tissue samples were close to the three-year field study by Gagnon et al., where no phosphorus was externally applied.

Notably, iron content in the roots and shoots was significantly ($p < 0.01$) higher at the midpoint in Fh-enriched systems than in control (Fig. S5).Higher Fh resulted in higher iron in roots with 1568 ± 88 μg g^{-1} (0.00% Fh), 1956 ± 60 μg g^{-1} (0.05% Fh), and 2325 ± 128 μg g^{-1} (0.10% Fh), and in shoots with 287 ± 37 μg g^{-1} (0.00% Fh), 377 ± 24 μg g^{-1} (0.05% Fh) and 575 ± 66 μg g^{-1} (0.10% Fh). At the endpoint, crops from Fh-enriched soils had significantly ($p < 0.01$) higher iron compared to control; however, iron concentrations in 0.05% and 0.10% Fh systems were similar (Fig. S5). Roots at endpoint contained 1134 ± 10 μg g^{-1} (0.00% Fh), 1382 ± 131 μg g^{-1} (0.05% Fh) and 1724 ± 197 μg g^{-1} (0.10% Fh) and shoots contained 5.28 ± 3.8 μg g^{-1} (0.00% Fh), 100.9 ± 3.3 μg g^{-1} (0.05% Fh) and 99.6 ± 2.4 μg g^{-1} (0.10% Fh). The kernels from Fh-enriched soils contained higher iron compared to control, which were 47.2 ± 11.6 μg g^{-1} (0.00% Fh), 78.2 ± 10.7 μg g^{-1} (0.05% Fh), and 85.2 ± 3.0 μg g^{-1} (0.10% Fh). The data suggests iron uptake and translocation by crops may reach a threshold, and with increasing soil Fh concentration, crops may downregulate uptake mechanisms to prevent iron toxicity. This iron uptake regulation is known to occur in

maize (Li et al., 2018; Roberts et al., 2004; Wairich et al., 2019; Zanin et al., 2017) and explains similar crop iron concentrations among Fh-enriched systems (Fig. S5).

In addition to improving nutrient use efficiency, Fh soil amendment seems to lower translocation of arsenic and uranium from shoot to grain (Fig. 2b). At endpoint, the transfer factor (TF) from shoot to grain for arsenic were 0.22 ± 0.02 (0.00% Fh), 0.20 ± 0.02 (0.05% Fh), 0.19 ± 0.01 (0.10% Fh), which did not vary significantly and for uranium were, 0.40 ± 0.01 (0.00% Fh), 0.37 ± 0.05 (0.05% Fh) and 0.29 ± 0.02 (0.10% Fh), which varied significantly ($p < 0.01$) for 0.10% Fh application. The endpoint TF observed for root to shoot (Fig. S6a, b) were 0.33 ± 0.02 (0.00% Fh), 0.29 ± 0.05 (0.05% Fh) and 0.26 ± 0.01 (0.10% Fh) for arsenic and 0.03 ± 0.004 (0.00% Fh), 0.02 ± 0.003 (0.05% Fh) and 0.016 ± 0.004 (0.10% Fh) for uranium where the differences were significant ($p < 0.01$). Compared to control, different crop tissues from Fh-enriched soils had lower concentrations of arsenic and uranium (Fig. 2c, d). The amount of arsenic present in shoot (0.00% Fh = 0.45 ± 0.06 μg g^{-1}; 0.05% Fh = 0.36 ± 0.04 μg g^{-1}; 0.10% Fh = 0.25 ± 0.04 μg g^{-1}) and grain (0.00% Fh = 0.10 ± 0.01 μg g^{-1}; 0.05% Fh = 0.07 ± 0.003 μg g^{-1}; 0.10% Fh = 0.05 ± 0.003 μg g^{-1}) at the endpoint was significantly ($p < 0.01$) lower for Fh-enriched systems compared to control (Fig. 2c). Arsenic in kernels was 0.1 μg g^{-1} in the control soil, which is the Food and Drug Administration (FDA) suggested limit for arsenic content in food grains (FDA, 2019). Arsenic and uranium uptake in maize grown in the control soil was comparable with previous studies (Rosas-Castor et al., 2014; Stojanović et al., 2016). The highest percentage of total arsenic and uranium was concentrated in the roots (Fig. S6c). Interestingly, at the endpoint, roots in Fh-enriched soils contained a higher percentage of arsenic and uranium (significant, $p < 0.01$) than control (Fig. S6c).

Uranium concentrations in shoot (0.00% Fh = 0.061 ± 0.013 μg g^{-1}; 0.05% Fh = 0.033 ± 0.008 μg g^{-1}; 0.10% Fh = 0.024 ± 0.005 μg g^{-1}) and grain (0.00% Fh = 0.024 ± 0.006 μg g^{-1}; 0.05% Fh = 0.012 ± 0.002 μg g^{-1} ; 0.10% Fh = 0.007 ± 0.002 μg g^{-1}) were significantly ($p<0.01$) lower in endpoint crops from Fh-enriched systems than in control (Fig. 2d). The amount of uranium in the shoot and grain was lower than arsenic due to low uranium mobility, as predicted by the model. Translocation of uranium from shoot to grain was higher than arsenic. However, elevated Fh significantly ($p < 0.01$) lowered the translocation rate (Fig. 2b). Uranium

translocation from root to shoot was lower than for arsenic. The presence of Fh may have further reduced this translocation (Fig. S6a, b). The lower concentration of trace elements in the kernels from Fh-enriched systems will help lower trace element concentration in the downstream food products and may protect human health as these contaminants are known for their toxicity. Further, increased iron concentration in kernels of Fh-enriched soil can aid in iron fortification in final products.

The bioaccumulation factor (BF) for arsenic was 1.0 (0.00% Fh), 0.8 (0.05% Fh), and 0.7 (0.10% Fh); and for uranium, 1.2 (0.00% Fh), 1.2 (0.05% Fh), and 1.2 (0.10% Fh) at midpoint. At the endpoint, the BF was 0.7 (0.00% Fh), 0.6 (0.05% Fh), and 0.5 (0.10% Fh) for arsenic; and 1.5 (0.00% Fh), 1.3 (0.05% Fh), and 1.2 (0.10% Fh) for uranium. The BF values at midpoint and reduction of translocation factor at endpoint suggests major uptake of trace contaminants occurred at the initial growth stage.

Higher uptake of trace contaminants at midpoint, specifically arsenic, seems to be influenced by elevated porewater Fe^{2+}. In graminaceous plants like maize, the primary iron uptake mechanism is chelation, not reduction (Bai et al., 2018; Roberts et al., 2004). However, maize can have a combined iron uptake mechanism where uptake can occur by chelation and by iron reduction pathway, especially under iron-deficient conditions (Li et al., 2018; Wairich et al., 2019; Zanin et al., 2017). Crop demand-driven iron uptake (Morrissey et al., 2009), coupled with higher availability of readily accessible iron in Fh-enriched soil will likely utilize the chelation pathway. However, under conditions of low plant-available iron, such as in control soil, both uptake mechanisms are possible. The dual uptake mechanisms of maize can explain elevated porewater Fe^{2+} and reduced arsenic in control compared to Fh-enriched systems. The combined effect of matching crop iron demand by both pathways and presence of anoxic microsites can explain a higher concentration of trace elements in the control crops than Fh-enriched systems. It seems evident that Fh's addition to unsaturated soils is beneficial to plants and very likely plays a vital role in the geochemistry at the rhizosphere.

3.3. Key aspects of ferrihydrite enrichment in the rhizosphere soil

DCB extractable iron concentration in the three soils on Day 0 were 614 ± 56, 822 ± 68, and 1125± 63 μg g^{-1} for control, 0.05%, and 0.10% Fh, respectively. The low variability of DCB extractable iron at Day 0 suggests

homogeneous Fh distribution in the top 5 cm soil. It was expected that Fh added to the soil will be easily accessible to the plants (Brown et al., 1991; Malakar et al., 2020) and preferentially used to fulfill crop iron demand, which is indicated by higher crop iron concentration in Fh-enriched systems (Fig. S5). Further, it was anticipated that the bulk soil composition would not be influenced by rhizosphere processes and should have a similar or slightly lower concentration, if Fh transformation occurs, of DCB extractable iron at mid- and endpoint, than Day 0. DCB extractable iron in bulk soil followed the expected pattern in 0.10% Fh at mid and endpoints (i.e., Day 45 and 105) (**Fig. 3**a). The predicted pattern was observed in the 0.05% Fh at the endpoint. However, DCB

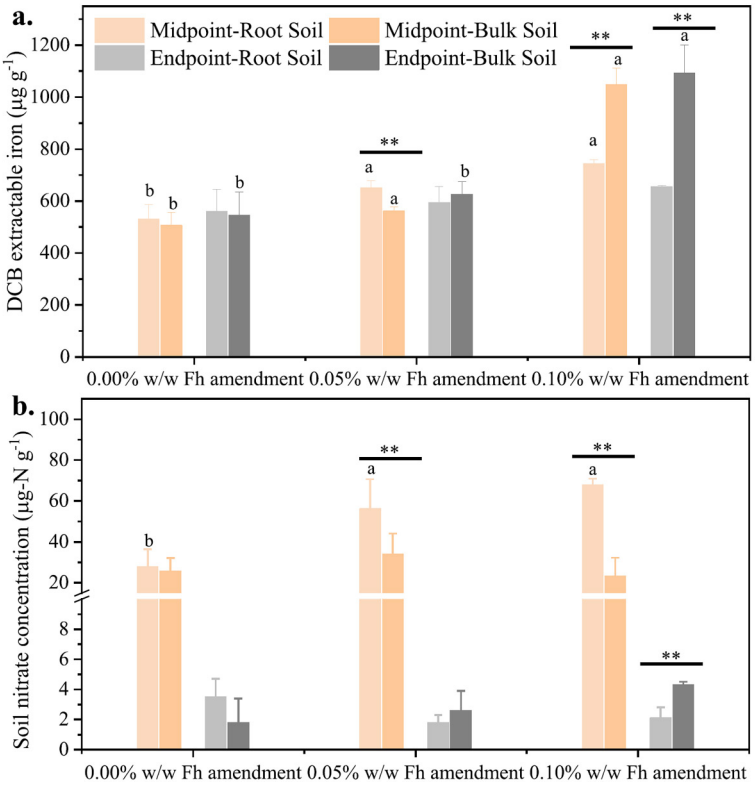

Fig. 3. Concentration of a. dithionite-citrate-bicarbonate (DCB) extractable iron, and b. soil nitrate among the three different Fh amended systems, at the rhizosphere soil and bulk soil for mid (Day 45) and endpoint (Day 105) of the experiment. The Y-axis has a break to show the entire dataset. Elevated level of Fh at the root zone promotes higher iron uptake by crops, therefore DCB extractable iron concentration at the root zone soil reduced considerably in Fh amended systems. Freshly added Fh enhances nitrate availability to the crops, with elevated levels of soil nitrate at the root zone. ** above vinculum (represent comparison between, root and bulk soil within same system), a and b show significantly different concentration between the treatments at $p < 0.01$ as per post hoc Tukey test. Bars without letter means interactions were not significant.

extractable iron was higher in rhizosphere soil of control (at mid- and endpoint) and 0.05% Fh (at midpoint) (Fig. 3a). In the 0.05% Fh, the difference in DCB extractable iron between rhizosphere and bulk soil was significantly ($p < 0.01$) different.

Iron demand in maize is higher in the initial growth stage (Xue et al., 2014), which may be the reason for higher DCB extractable iron in rhizosphere soils of control and 0.05% Fh (DCB extractable iron, control: 530± 56 μg g^{-1}, 0.05% Fh: 651 ± 28 μg g^{-1}, 0.10% Fh: 744 ± 16 μg g^{-1}). The elevated concentration of DCB extractable iron in control and 0.05% Fh systems may indicate preferential extractable iron enrichment at the rhizosphere tied to the crop iron demand, which is regulated by maize roots as per soil iron availability (Li et al., 2018; Roberts et al., 2004; Wairich et al., 2019; Zanin et al., 2017). A similar mechanism of preferential iron enrichment may occur in the rhizosphere of the 0.10% Fh system. However, given the elevated levels of externally supplied Fh, as soon as the crop iron demand is fulfilled, crops downregulate iron uptake (Li et al., 2018; Roberts et al., 2004; Wairich et al., 2019; Zanin et al., 2017). The downregulation of iron uptake may be a reason for low or no extractable iron enrichment at the rhizosphere soil of 0.10% Fh. The model predicted Fh's saturation indices at Day 90 porewater suggested fresh Fh precipitation, which explains higher DCB extractable iron in control at the endpoint. Crops typically require less iron at later growth stages (Xue et al., 2014), which may be why at the endpoint, DCB extractable iron in rhizosphere soil of Fh-enriched systems does not decrease much from the midpoint. Colloidal particles, such as Fh, can be transported along with the mass flow in the soil (Bagheri et al., 2019; Bradford et al., 2002; Kretzschmar and Schafer, 2005), as per plant water demand. The concentration of total (average of root and bulk soil) arsenic and uranium slightly increased by the end of the experiment (Table S3), which may be within the variability of the soil. Further, as the experiment progressed, Fh's higher availability in amended soil may bound arsenic and uranium coming from irrigation water within the soil (Kobayashi et al., 2020; Malakar et al., 2021; Tong et al., 2020) and makes them less available to the crops or leaching to the porewater table.

Soil water content, a critical component for plant growth, was positively influenced by Fh addition. Throughout the experiment, Fh-enriched soils had significantly ($p < 0.01$) higher water retention. Average gravimetric soilwater content (Fig. S2)was 12.8±1.5% for the control,

15.4 ± 1.9% for 0.05% Fh, and 17.1 ± 2.2% for 0.10% Fh. The unsatisfied bonds on Fh's surface (Weatherill et al., 2016), may help retain water molecules efficiently and increase the soilwater content. Further, the Fh amendment aided in nutrient use efficiency by the preferential distribution of nutrients in the soil, another key feature for promoting plant growth. At the midpoint when nitrate demand was high, rhizosphere soil of the Fh-enriched system had significantly ($p < 0.01$) higher nitrate concentration than control (Fig. 3b). The 0.10% Fh treatment had the highest nitrate concentration (67.9 ± 3.0 μg-N g^{-1}) followed by 0.05% Fh (56.2 ± 4.5 μg-N g^{-1}), and control (27.7 ± 8.8 μg-N g^{-1}). The bulk soil nitrate concentration was comparable to rhizosphere soil (25.7 ± 6.4 μg-N g^{-1}) in control, but in the Fh-enriched systems, bulk soil had significantly lower nitrate (33.9 ± 10.1 μg-N g^{-1}, 0.05% Fh; 23.4 ± 8.8 μg-N g^{-1}, 0.10% Fh). Maize nitrogen demand is highest during the initial growth stage (Mengel and Barber, 1974; Olness and Beoit, 1992), and a higher nitrate level at rhizosphere would improve crop health. At the endpoint, 0.10% Fh showed significantly ($p < 0.01$) lower nitrate concentration in rhizosphere soil than the bulk. This lower nitrate in rhizosphere may be due to better utilization of nitrate by the crops. The lower concentrations of nitrate in porewater of Fh-enriched soils indicated better nitrate retention in the soil, and soil nitrate data affirms that. The distribution of soil nitrate indicates that Fh enrichment may facilitate plant nitrate use efficiency as reflected by relative chlorophyll content. Phosphorous concentrations in soil were similar between the root and bulk soil (Fig. S7).

Nitrate can bind to Fh by monodentate mononuclear surface complexation through normal or charge-assisted hydrogen bonding (Acelas et al., 2017). The adsorption of nitrate on fresh Fh can lower nitrate loss and make them more available at the rhizosphere during preferential movement of Fh towards the rhizosphere. High iron demand at the midpoint explains the higher nitrate concentration at the rhizosphere, which aided in plant growth. Fh is known to interact with dissolved phosphate (Rhoton and Bigham, 2005; van Veelen et al., 2019), and iron oxides present in soil from the beginning could have already adsorbed phosphate, and phosphate was not supplied externally in the experiment. Low doses of added Fh were not found to affect phosphorus plant availability as indicated by phosphorus concentration in crops. The enhanced availability of soil water and efficient nutrient distribution positively influenced plant growth in Fh-enriched soils.

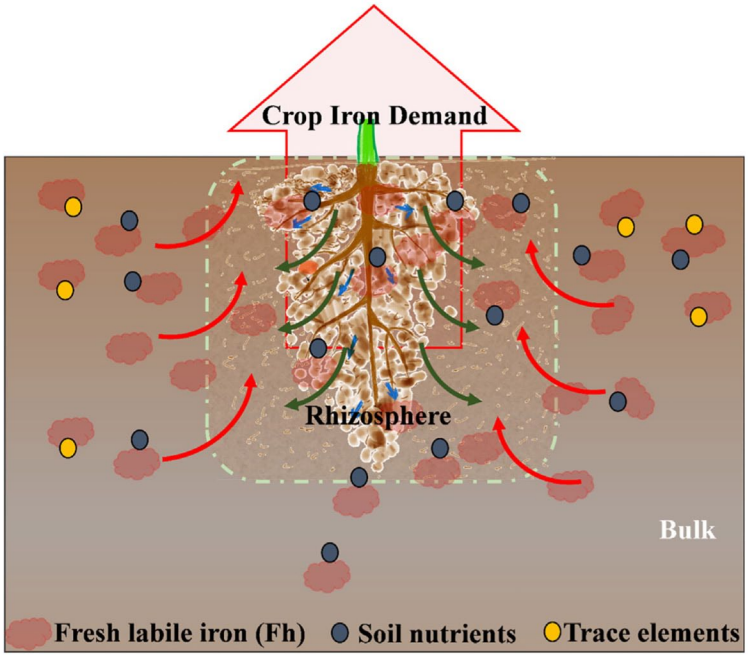

Fig. 4. Predicted role of iron nanominerals or ferrihydrite (Fh (red)) enrichment at the root zone soil. Availability of easily accessible iron source in the soil enhances crop iron uptake, primarily by chelation. Elevated levels of iron at the root zone-soil-porewater interface intensifies root zone processes (green arrow) such as release of exudates for chelation, which may further drive the preferential enrichment of Fh nanomineral to the interface of root zone (red arrows). The directed flow elevates levels of Fh in the root zone, also makes nutrients (blue dots) such as nitrate (added on day 7 after Fh amendment), concentrated at the vicinity of roots, enhancing plant biomass, and health indices. Further, nanomineral present in the soil of the unsaturated zone, helps in limiting movement of trace contaminants (yellow dots) such as arsenic and uranium coming periodically from irrigation water, and preferentially retains nutrients and moisture.

Elucidating the effects of Fh addition to unsaturated agricultural soil is the primary outcome of the present study. The positive influence on plant nutrient availability and trace contaminants attenuation is a consequence of elevated Fh nanomineral in the unsaturated soil (**Fig. 4**). Our results highlight how the dynamics of reactive iron minerals influenced by crop iron demand, and flow of porewater in irrigated soil, can control the accessibility of nutrients and attenuation of trace elements. The percolation of irrigation water through the soil pores and subsequent water movement to the roots seem to promote movement of colloidal Fh (Bagheri et al., 2019; Bradford et al., 2002; Kretzschmar and Schafer, 2005). Our data showed that Fh in the root zone-soil-porewater interface is an

essential factor controlling nutrient and trace element bioavailability in transiently saturated irrigated soils. Anoxic microsites in the root zone-soil-porewater interface of unsaturated soil may regulate important redox-sensitive reactions (Malakar et al., 2020). Further, the availability of labile iron mineral at the vicinity of these microsites seems to play a critical role in controlling geochemical reactions favoring plant growth and limiting trace contaminants mobility.

While the Fh enrichment was carried out in a controlled greenhouse experiment, subsequent experiments under actual field conditions are needed to validate this study's results. The study contributes to a better understanding of the critical role that iron nanominerals play in irrigated unsaturated soil and provides a framework for future field studies to improve management for better nutrient and moisture availability to crops grown under these conditions. Addition of low doses of iron nanominerals to soils under sprinkler or subsurface drip irrigation can have significant implications for accessibility of nutrients, including iron, and control trace element mobilization. Fh amendments may also beneficially manage biogeochemical cycles of carbon and nitrogen at the rhizosphere. These critical processes controlled by iron nanominerals under unsaturated conditions need to be further clarified and quantified as nutrients and contaminants lost from the root zone can infiltrate into the groundwater. Finally, the role of natural and synthetic iron nanominerals under unsaturated irrigated soils seems to be crucial for improving water and food safety and security.

* * * *

CRediT authorship contribution statement

Arindam Malakar: Conceptualization, Methodology, Visualization, Data curation, Investigation, Validation, Formal analysis, Writing – original draft.
Daniel D. Snow: Methodology, Supervision, Data curation, Resources, Validation, Project administration, Writing – review & editing.
Michael Kaiser: Methodology, Visualization, Validation, Formal analysis, Supervision, Writing – review & editing.
Jordan Shields: Investigation, Data curation, Writing – review & editing.
Bijesh Maharjan: Resources, Writing – review & editing.
Harkamal Walia: Methodology, Writing – review & editing.
Daran Rudnick: Writing – review & editing.
Chittaranjan Ray: Methodology, Supervision, Project administration, Funding acquisition, Writing – review & editing.

Competing interests The authors declare that they have no known competing financial interest or personal relationships that could have appeared to influence the work reported in this paper.

Acknowledgments This work was partially supported by the Nebraska Agricultural Experiment Station with funding from the Hatch Multistate Research (Accession Number 1011588) through the USDA National Institute of Food and Agriculture. The research was performed in part in the Nebraska Nanoscale Facility: National Nanotechnology Coordinated Infrastructure and the Nebraska Center for Materials and Nanoscience, which are supported by the National Science Foundation under Award ECCS:2025298 and the Nebraska Research Initiative. Authors thank Water Sciences Laboratory at University of Nebraska Lincoln, for helping with analyses of samples.

Appendix A. Supplementary data The supplementary data (word document) contains additional details of the materials and method section. Fig. S1, shows x-ray diffraction of synthesize 2-line ferrihydrite. Fig. S2, shows temporal gravimetric moisture content variation; Fig. S3, shows the temporal variation in relative chlorophyll content in crops and temporal variation in crop height; Fig. S4, shows plant shoot and root pictures from the greenhouse; Fig. S5, shows the concentration of iron in roots, shoots and grains of crops under three different treatment regime; Fig. S6, translocation of arsenic and uranium within the crops and shows percentage of arsenic and uranium content in the grains and roots of endpoint crops; Fig. S7, shows soil total phosphorus at the root and bulk soil of the three treatments; Table S1, compares experimental arsenate values with aqueous speciation model predicted values; Table S2, compares experimental reduced iron values with aqueous speciation model predicted values, and Table S3 shows total arsenic and uranium concentration in soils. Supplementary data to this article is attached to its archive record.

References

Acelas, N.Y., Hadad, C., Restrepo, A., Ibarguen, C., Flórez, E., 2017. Adsorption of nitrate and bicarbonate on Fe-(Hydr)oxide. Inorg. Chem. 56, 5455–5464. https://doi.org/10.1021/acs.inorgchem.7b00513

Amaral, D.C., Lopes, G., Guilherme, L.R.G., Seyfferth, A.L., 2017. A new approach to sampling intact Fe plaque reveals Si-induced changes in Fe mineral composition and shoot as in Rice. Environ. Sci. Technol. 51, 38–45. https://doi.org/10.1021/acs.est.6b03558

Appelo, C.A.J., Van Der Weiden, M.J.J., Tournassat, C., Charlet, L., 2002. Surface complexation of ferrous iron and carbonate on ferrihydrite and the mobilization of arsenic. Environ. Sci. Technol. 36, 3096–3103. https://doi.org/10.1021/es010130n

Bagheri, H., Zare Abyaneh, H., Izady, A., Brusseau, M.L., 2019. Modeling the transport of nitrate and natural multi-sized colloids in natural soil and soil amended with vermicompost. Geoderma 354, 113889. https://doi.org/10.1016/j.geoderma.2019.113889

Bai, G., Jenkins, S., Yuan, W., Graef, G.L., Ge, Y., 2018. Field-based scoring of soybean iron deficiency chlorosis using RGB imaging and statistical learning. Front. Plant Sci. 9, 1002. https://doi.org/10.3389/fpls.2018.01002

Ball, J.W., Nordstrom, D.K., 1991. User's manual for WATEQ4F, with revised thermodynamic data base and text cases for calculating speciation of major, trace, and redox elements in natural waters. Open-File Report 91-183 https://doi.org/10.3133/ofr91183

Boghi, A., Roose, T., Kirk, G.J.D., 2018. A model of uranium uptake by plant roots allowing for root-induced changes in the soil. Environ. Sci. Technol. 52, 3536–3545. https://doi.org/10.1021/acs.est.7b06136

Borch, T., Kretzschmar, R., Kappler, A., Cappellen, P. Van, Ginder-Vogel, M., Voegelin, A., Campbell, K., 2010. Biogeochemical redox processes and their impact on contaminant dynamics. Environ. Sci. Technol. 44, 15–23. https://doi.org/10.1021/es9026248

Bowman, J.A., Simmons, F.W., Kimpel, B.C., 1991. Irrigation in midwest: lessons from Illinois. J. Irrig. Drain. Eng. 117 (5), 700–715. https://doi.org/10.1061/(ASCE)0733-9437(1991)117:5(700)

Bradford, S.A., Yates, S.R., Bettahar, M., Simunek, J., 2002. Physical factors affecting the transport and fate of colloids in saturated porous media. Water Resour. Res. 38, 63- 1–63–12. https://doi.org/10.1029/2002WR001340

Brown, J.C., Von Jolley, D., Lytle, C.M., 1991. Comparative evaluation of iron solubilizing substances (phytosiderophores) released by oats and corn: iron-efficient and iron-inefficient plants. Plant Soil 130, 157–163. https://doi.org/10.1007/BF00011870

Bundschuh, J., Nath, B., Bhattacharya, P., Liu, C.W., Armienta, M.A., Moreno López, M.V., Lopez, D.L., Jean, J.S., Cornejo, L., Lauer Macedo, L.F., Filho, A.T., 2012. Arsenic in the human food chain: the Latin cameraman perspective. Sci. Total Environ. 429, 92–106. https://doi.org/10.1016/j.scitotenv.2011.09.069

Colombo, C., Palumbo, G., He, J.Z., Pinton, R., Cesco, S., 2014. Review on iron availability in soil: interaction of Fe minerals, plants, and microbes. J. Soils Sediments 14, 538–548. https://doi.org/10.1007/s11368-013-0814-z

Cornell, R.M., 1988. The influence of some divalent cations on the transformation of ferrihydrite to more crystalline products. Clay Miner. 23, 329–332. https://doi.org/10.1180/claymin.1988.023.3.10

Cornell, R.M., Schwertmann, U., 2003. The Iron Oxides: Structure, Properties, Reactions, Occurences and Uses, Second Edition. Second. ed. WILEY-VCH GmbH & Co. KGaA. Wiley https://doi.org/10.1002/3527602097

Coward, E.K., Thompson, A., Plante, A.F., 2018. Contrasting Fe speciation in two humid forest soils: insight into organomineral associations in redox-active environments. Geochim. Cosmochim. Acta 238, 68–84. https://doi.org/10.1016/j.gca.2018.07.007

Das, S., Hendry, M.J., Essilfie-Dughan, J., 2011a. Transformation of two-line ferrihydrite to goethite and hematite as a function of pH and temperature. Environ. Sci. Technol. 45, 268–275. https://doi.org/10.1021/es101903y

Das, S., Hendry, M.J., Essilfie-Dughan, J., 2011b. Effects of adsorbed arsenate on the rate of transformation of 2-line ferrihydrite at pH 10. Environ. Sci. Technol. 45, 5557–5563. https://doi.org/10.1021/es200107m

Deng, Q., Hui, D., Wang, J., Iwuozo, S., Yu, C.L., Jima, T., Smart, D., Reddy, C., Dennis, S., 2015. Corn yield and soil nitrous oxide emission under different fertilizer and soil management: a three-year field experiment in middle Tennessee. PLoS One 10 (4), e0125406. https://doi.org/10.1371/journal.pone.0125406

Dieter, C.A.A., Maupin, M.A.A., Caldwell, R.R.R., Harris, M.A.A., Ivahnenko, T.I.I., Lovelace, J.K.K., Barber, N.L.L., Linsey, K.S.S., 2018. Estimated Use of Water in the United States in 2015: U.S. Geological Survey Circular 1441. U.S. Geological Survey https://doi.org/10.3133/cir1441

Dietrich, S., Bea, S.A., Weinzettel, P., Torres, E., Ayora, C., 2016. Occurrence and distribution of arsenic in the sediments of a carbonate-rich unsaturated zone. Environ. Earth Sci. 75, 1–14. https://doi.org/10.1007/s12665-015-4892-7

Elder, J.A., 1969. Soils of Nebraska. Conservation and Survey Division, University of Nebraska. Lincoln, p. 60. https://digitalcommons.unl.edu/conservationsurvey/444/

FDA, 2019. Arsenic in food and dietary supplements | FDA [WWW Document]. https://www.fda.gov/food/metals/arsenic-food-and-dietary-supplements. (Accessed 8 July 2019).

Freeman, K.W., Girma, K., Arnall, D.B., Mullen, R.W., Martin, K.L., Teal, R.K., Raun, W.R., 2007. By-plant prediction of corn forage biomass and nitrogen uptake at various growth stages using remote sensing and plant height. Agron. J. 99, 530–536. https://doi.org/10.2134/agronj2006.0135

Gagnon, B., Ziadi, N., Bélanger, G., Parent, G., 2020. Validation and use of critical phosphorus concentration in maize. Eur. J. Agron. 120, 126147. https://doi.org/10.1016/j.eja.2020.126147

Gmach, M.R., Cherubin, M.R., Kaiser, K., Cerri, C.E.P., 2020. Processes that influence dissolved organic matter in the soil: a review. Sci. Agric. 77 (3), e20180164. https://doi.org/10.1590/1678-992x-2018-0164

Green, C.T., Fisher, L.H., Bekins, B.A., 2008. Nitrogen fluxes through unsaturated zones in five agricultural settings across the United States. J. Environ. Qual. 37, 1073–1085. https://doi.org/10.2134/jeq2007.0010

Gypser, S., Hirsch, F., Schleicher, A.M., Freese, D., 2018. Impact of crystalline and amorphous iron- and aluminum hydroxides on mechanisms of phosphate adsorption and desorption. J. Environ. Sci. 70, 175–189. https://doi.org/10.1016/j.jes.2017.12.001

Hall, S.J., Silver, W.L., 2015. Reducing conditions, reactive metals, and their interactions can explain spatial patterns of surface soil carbon in a humid tropical forest. Biogeochemistry 125, 149–165. https://doi.org/10.1007/s10533-015-0120-5

Han, L., Sun, K., Keiluweit, M., Yang, Yu., Yang, Yan, Jin, J., Sun, H., Wu, F., Xing, B., 2019. Mobilization of ferrihydrite-associated organic carbon during Fe reduction: adsorption versus coprecipitation. Chem. Geol. 503, 61–68. https://doi.org/10.1016/j.chemgeo.2018.10.028

Heikens, A., Panaullah, G.M., Meharg, A.A., 2007. Arsenic behaviour from groundwater and soil to crops: impacts on agriculture and food safety. Rev. Environ. Contam. Toxicol. 189, 43–87. https://doi.org/10.1007/978-0-387-35368-5_3

Hoagland, D.R., Arnon, D.I., 1950. The water-culture method for growing plants without soil. Circular. California Agricultural Experiment Station, p. 347.

Hu, S., Lu, Y., Peng, L., Wang, P., Zhu, M., Dohnalkova, A.C., Chen, H., Lin, Z., Dang, Z., Shi, Z., 2018. Coupled kinetics of ferrihydrite transformation and As(V) sequestration under the effect of humic acids: a mechanistic and quantitative study. Environ. Sci. Technol. 52, 11632–11641. https://doi.org/10.1021/acs.est.8b03492

Irmak, S., Haman, D.Z., Bastug, R., 2000. Determination of crop water stress index for irrigation timing and yield estimation of corn. Agron. J. 92 (6), 1221–1227. https://doi.org/10.2134/agronj2000.9261221x

Islam, S., Das, S., Mishra, G., Das, B., Malakar, A., Carlomagno, I., Meneghini, C., De Giudici, G., Gonçalves, L.P.L., Sousa, J.P.S., Kolen'ko, Y.V., Kuncser, A.C., Ray, S., 2020. . Coagulating and flocculating ferrihydrite: application of zinc acetate salt. Environ. Sci. Water Res. Technol. 6, 2057–2064. https://doi.org/10.1039/D0EW00357C

Jambor, J.L., Dutrizac, J.E., 1998. Occurrence and constitution of natural and synthetic ferrihydrite, a widespread iron oxyhydroxide. Chem. Rev. 98, 2549–2586. https://doi.org/10.1021/cr970105t

Jang, J.-H., Dempsey, B.A., Catchen, G.L., Burgos, W.D., 2003. Effects of Zn(II), Cu(II), Mn(II), Fe(II), NO^{3-}, or SO_4^{2-} at pH 6.5 and 8.5 on transformations of hydrous ferric oxide (HFO) as evidenced by Mössbauer spectroscopy. Colloids Surfaces A Physicochem. Eng. Asp. 221, 55–68. https://doi.org/10.1016/S0927-7757(03)00134-1

Kaifer, A.E., 1992. In: Skoog, Douglas A., West, Donald M., Hollar, James F. (Eds.), Fundamentals of Analytical Chemistry, Sixth edition, Journal of Chemical Education, p. A305 https://doi.org/10.1021/ed069pa305.1

Keiluweit, M., Wanzek, T., Kleber, M., et al., 2017. Anaerobic microsites have an unaccounted role in soil carbon stabilization. Nat. Commun. 8, 1771. https://doi.org/10.1038/s41467-017-01406-6

Kobayashi, Y., Fukushi, K., Kosugi, S., 2020. A robust model for prediction of U(VI) adsorption onto ferrihydrite consistent with spectroscopic observations. Environ. Sci. Technol. 54, 2304–2313. https://doi.org/10.1021/acs.est.9b06556

Kölling, M., 2000. Comparison of different methods for redox potential determination in natural waters. Redox. Springer, Berlin Heidelberg, pp. 42–54 https://doi.org/10.1007/978-3-662-04080-5_4

Kretzschmar, R., Schafer, T., 2005. Metal retention and transport on colloidal particles in the environment. Elements 1, 205–210. https://doi.org/10.2113/gselements.1.4.205

Kutscher, D.J., McSheehy-Ducos, S., Wills, J., Jensen, D., 2012. IC-ICP-MS speciation analysis of As in apple juice using the Thermo Scientific iCAP Q ICP-MSNo. 43099.

Li, S., Zhou, X., Chen, J., Chen, R., 2018. Is there a strategy I iron uptake mechanism in maize? Plant Signal. Behav. 13, e1161877. https://doi.org/10.1080/15592324.2016 1161877.

Link, D.D., Walter, P.J., Kingston, H.M., 1998. Development and validation of the new EPA microwave-assisted leach method 3051A. Environ. Sci. Technol. 32, 3628–3632. https://doi.org/10.1021/es980559n

Malakar, A., Das, B., Islam, S., Meneghini, C., De Giudici, G., Merlini, M., Kolen'ko, Y.V., Iadecola, A., Aquilanti, G., Acharya, S., Ray, S., 2016a. Efficient artificial mineralization route to decontaminate Arsenic(III) polluted water - the Tooeleite Way. Sci. Rep. 6, 26031. https://doi.org/10.1038/srep26031

Malakar, A., Islam, S., Ali, M.A., Ray, S., 2016b. Rapid decadal evolution in the groundwater arsenic content of Kolkata, India and its correlation with the practices of her dwellers. Environ. Monit. Assess. 188, 1–22. https://doi.org/10.1007/s10661-016-5592-9

Malakar, A., Snow, D.D., Ray, C., 2019. Irrigation water quality-a contemporary perspective. Water 11, 1482. https://doi.org/10.3390/w11071482

Malakar, A., Kaiser, M., Snow, D.D., Walia, H., Panda, B., Ray, C., 2020. Ferrihydrite reduction increases arsenic and uranium bioavailability in unsaturated soil. Environ. Sci. Technol. 54, 13839–13848. https://doi.org/10.1021/acs.est.0c02670

Malakar, A., Singh, R., Westrop, J., Weber, K.A., Elofson, C.N., Kumar, M., Snow, D.D., 2021. Occurrence of arsenite in surface and groundwater associated with a perennial stream located in Western Nebraska, USA. J. Hazard. Mater. 416, 126170. https://doi.org/10.1016/j.jhazmat.2021.126170

Mariotti, M., Ercoli, L., Masoni, A., 1996. Spectral properties of iron-deficient corn and sunflower leaves. Remote Sens. Environ. 58, 282–288. https://doi.org/10.1016/S0034-4257(96)00070-3

Mengel, D.B., Barber, S.A., 1974. Rate of nutrient uptake per unit of corn root under field conditions. Agron. J. 66, 399–402. https://doi.org/10.2134/agronj1974.00021962006600030019x

Michel, F.M., Ehm, L., Antao, S.M., Lee, P.L., Chupas, P.J., Liu, G., Strongin, D.R., Schoonen, M.A.A., Phillips, B.L., Parise, J.B., 2007. The structure of ferrihydrite, a nanocrystalline material. 316, 1726–1729. https://doi.org/10.1126/science.1142525

Morrissey, J., Guerinot, M. Lou, Morrissey, J., Guerinot, M.Lou, 2009. Iron uptake and transport in plants: the good, the bad, and the ionome. Chem. Rev. 109, 4553–4567. https://doi.org/10.1021/cr900112r

Nordstrom, D.K., Plummer, L.N., Wigley, T.M.L., Wolery, T.J., Ball, J.W., Jenne, E.A., Bassett, R.L., Crerar, D.A., Florence, T.M., Fritz, B., Hoffman, M., Holdren, G.R., Lafon, G.M., Mattigod, S.V., McDuff, R.E., Morel, F., Reddy, M.M., Sposito, G., Thrailkill, J., 1979. A comparison of computerized chemical models for equilibrium calculations in aqueous systems. In: Jene, E.A. (Ed.), Chemical Modeling in Aqueous Systems. American Chemical Society, pp. 857–892 https://doi.org/10.1021/bk-1979-0093.ch038

O'Rourke, J.A., Charlson, D.V., Gonzalez, D.O., Vodkin, L.O., Graham, M.A., Cianzio, S.R., Grusak, M.A., Shoemaker, R.C., 2007. Microarray analysis of iron deficiency chlorosis in near-isogenic soybean lines. BMC Genomics 8, 476. https://doi.org/10.1186/1471-2164-8-476

Oliveira, S.M., Lopes, T.I.M.S., Rangel, A.O.S.S., 2006. Spectrophotometric determination of nitrite and nitrate in cured meat by sequential injection analysis. J. Food Sci. 69, C690–C695. https://doi.org/10.1111/j.1365-2621.2004.tb09917.x

Olness, A., Beoit, G.R., 1992. A closer look at corn nutrient demand. Better Crops With Plant Food. 76, pp. 18–20. http://www.ipni.net/publication/bettercrops.nsf/0/A61B8AEDECC1B25885257D33006A4C6A/$FILE/%20BC-1992-1%20p18.pdf

Parkhurst, D.L., Appelo, C.A.J., 2013. PHREEQC (Version 3)-a computer program for speciation, batch-reaction, one-dimensional transport, and inverse geochemical calculations. Model. Tech. B. 6, 497. https://www.usgs.gov/software/phreeqc-version-3

Perez, J.P.H., Tobler, D.J., Thomas, A.N., Freeman, H.M., Dideriksen, K., Radnik, J., Benning, L.G., 2019. Adsorption and reduction of arsenate during the Fe^{2+}-induced transformation of ferrihydrite. ACS Earth Space Chem. 3, 884–894. https://doi.org/10.1021/acsearthspacechem.9b00031

Rhoton, F.E., Bigham, J.M., 2005. Phosphate adsorption by ferrihydrite-amended soils. J. Environ. Qual. 34, 890. https://doi.org/10.2134/jeq2004.0176

Ritter, K., Aiken, G.R., Ranville, J.F., Bauer, M., Macalady, D.L., 2006. Evidence for the aquatic binding of arsenate by natural organic Matter–Suspended Fe(III). Environ. Sci. Technol. 40, 5380–5387. https://doi.org/10.1021/es0519334

Roberts, L.A., Pierson, A.J., Panaviene, Z., Walker, E.L., 2004. YellowStripe1. Expanded roles for the maize iron-phytosiderophore transporter. Plant Physiol. 135, 112–120. https://doi.org/10.1104/pp.103.037572

Rosas-Castor, J.M., Guzmán-Mar, J.L., Hernández-Ramírez, A., Garza-González, M.T., Hinojosa-Reyes, L., 2014. Arsenic accumulation in maize crop (*Zea mays*): a review. Sci. Total Environ. 488, 176–187. https://doi.org/10.1016/j.scitotenv.2014.04.075

Schwertmann, U., 1983. Effect of pH on the formation of goethite and hematite from ferrihydrite. Clay Clay Miner. 31, 277–284. https://doi.org/10.1346/CCMN.1983.0310405

Schwertmann, U., Stanjek, H., Becher, H.-H., 2004. Long-term in vitro transformation of 2- line ferrihydrite to goethite/hematite at 4, 10, 15 and 25°C. Clay Miner. 39, 433–438. https://doi.org/10.1180/0009855043940145

Shaw, S., 2005. The kinetics and mechanisms of goethite and hematite crystallization under alkaline conditions, and in the presence of phosphate. Am. Mineral. 90, 1852–1860. https://doi.org/10.2138/am.2005.1757

Sherman, D.M., Randall, S.R., 2003. Surface complexation of arsenic(V) to iron(III) (hydr) oxides: structural mechanism from ab initio molecular geometries and EXAFS spectroscopy. Geochim. Cosmochim. Acta 67, 4223–4230. https://doi.org/10.1016/S0016-7037(03)00237-0

Shi, G., Lu, H., Liu, H., Lou, L., Zhang, P., Song, G., Zhou, H., Ma, H., 2020. Sulfate application decreases translocation of arsenic and cadmium within wheat (*Triticum aestivum* L.) plant. Sci. Total Environ. 713, 136665. https://doi.org/10.1016/j.scitotenv.2020.136665

Smith, D.B., Cannon, W.F., Woodruff, L.G., 2011. A national-scale geochemical and mineralogical survey of soils of the conterminous United States. Appl. Geochemistry 26, S250–S255. https://doi.org/10.1016/j.apgeochem.2011.03.116

Smith, D.B., Cannon, W.F., Woodruff, L.G., Solano, F., Kilburn, J.E., Fey, D.L., 2013a. Geochemical and Mineralogical Data for Soils of the Conterminous United States, U.S. Geological Survey Data Series. Virginia. https://doi.org/10.3133/ds801

Smith, D.B., Smith, S.M., Horton, J.D., 2013b. History and evaluation of national-scale geochemical data sets for the United States. Geosci. Front. 4, 167–183. https://doi.org/10.1016/j.gsf.2012.07.002

Sparks, D.L., 2003. Inorganic Soil Components. Environmental Soil Chemistry. Elsevier, pp. 43–73 https://doi.org/10.1016/b978-012656446-4/50002-5

Stojanović, M., Pezo, L., Lačnjevac, Č., Mihajlović, M., Petrović, J., Milojković, J., Stanojević, M., 2016. Biometric approach in selecting plants for phytoaccumulation of uranium. Int. J. Phytoremediation 18, 527–533. https://doi.org/10.1080/15226514.2015.1115966

Tamura, H., Goto, K., Yotsuyanagi, T., Nagayama, M., 1974. Spectrophotometric determination of iron(II) with 1,10-phenanthroline in the presence of large amounts of iron(III). Talanta 21, 314–318. https://doi.org/10.1016/0039-9140(74)80012-3

Tong, J., Li, R., Zhang, J., Ma, X., Wu, F., Suo, H., Liu, C., 2020. Coupled dynamics of As-containing ferrihydrite transformation and As desorption/re-adsorption in presence of sulfide. J. Hazard. Mater. 384, 121287. https://doi.org/10.1016/j.jhazmat.2019.121287

United States Environmental Protection Agency (EPA), 1996. Method 3052: Microwave Assisted Acid Digestion of Siliceous and Organically Based Matrices. https://www.epa.gov/sites/default/files/2015-12/documents/3052.pdf

Van Groeningen, N., Thomas Arrigo, L.K., Byrne, J.M., Kappler, A., Christl, I., Kretzschmar, R., 2020. Interactions of ferrous iron with clay mineral surfaces during sorption and subsequent oxidation. Environ. Sci. Process. Impacts 22, 1355–1367. https://doi.org/10.1039/D0EM00063A

van Veelen, A., Koebernick, N., Scotson, C.S., McKay-Fletcher, D., Huthwelker, T., Borca, C.N., Mosselmans, J.F.W., Roose, T., 2019. Root-induced soil deformation influences Fe, S and P: rhizosphere chemistry investigated using synchrotron XRF and XANES. New Phytol. 225 (4), 1476–1490. https://doi.org/10.1111/nph.16242

Vodyanitskii, Y.N., 2011. Chemical aspects of uranium behavior in soils: a review. Eurasian Soil Sci. 44, 862–873. https://doi.org/10.1134/S1064229311080163

Vodyanitskii, Y.N., Shoba, S.A., 2016. Ferrihydrite in soils. Eurasian Soil Sci. 49, 796–806. https://doi.org/10.1134/S1064229316070127

Vu, H.P., Shaw, S., Brinza, L., Benning, L.G., 2010. Crystallization of hematite (α-Fe_2O_3) under alkaline condition: the effects of Pb. Cryst. Growth Des. 10, 1544–1551. https://doi.org/10.1021/cg900782g

Wagner, D., 2017. Effect of varying soil water potentials on methanogenesis in aerated marshland soils. Sci. Rep. 7, 14706. https://doi.org/10.1038/s41598-017-14980-y

Wairich, A., de Oliveira, B.H.N., Arend, E.B., Duarte, G.L., Ponte, L.R., Sperotto, R.A., Ricachenevsky, F.K., Fett, J.P., 2019. The combined strategy for iron uptake is not exclusive to domesticated rice (Oryza sativa). Sci. Rep. 9, 16144. https://doi.org/10.1038/s41598-019-52502-0

Wang, X., Li, W., Harrington, R., Liu, F., Parise, J.B., Feng, X., Sparks, D.L., 2013. Effect of ferrihydrite crystallite size on phosphate adsorption reactivity. Environ. Sci. Technol. 47, 10322–10331. https://doi.org/10.1021/es401301z

Wang, S., Wu, W., Liu, F., Liao, R., Hu, Y., 2017. Accumulation of heavy metals in soil-crop systems: a review for wheat and corn. Environ. Sci. Pollut. Res. 24, 15209–15225. https://doi.org/10.1007/s11356-017-8909-5

Weatherill, J.S., Morris, K., Bots, P., Stawski, T.M., Janssen, A., Abrahamsen, L., Blackham, R., Shaw, S., 2016. Ferrihydrite formation: the role of Fe_{13} keggin clusters. Environ. Sci. Technol. 50, 9333–9342. https://doi.org/10.1021/acs.est.6b02481

Wedepohl, K.H., 1991. Chemical composition and fractionation of the continental crust. Geol. Rundsch. 80, 207–223. https://doi.org/10.1007/BF01829361

Xue, Y., Yue, S., Zhang, W., Liu, D., Cui, Z., Chen, X., Ye, Y., Zou, C., 2014. Zinc, iron, manganese and copper uptake requirement in response to nitrogen supply and the increased grain yield of summer maize. PLoS One 9, e93895. https://doi.org/10.1371/journal.pone.0093895

Yang, W.H., Weber, K.A., Silver, W.L., 2012. Nitrogen loss from soil through anaerobic ammonium oxidation coupled to iron reduction. Nat. Geosci. 5, 538–541. https://doi.org/10.1038/ngeo1530

Yashim, Z.I., Kehinde Israel, O., Hannatu, M., 2014. A study of the uptake of heavy metals by plants near metal-scrap dumpsite in Zaria, Nigeria. J. Appl. Chem. 13 (3), 394650. https://doi.org/10.1155/2014/394650

Yu, X., Liu, C., Guo, Y., Deng, T., 2019. Speciation analysis of trace arsenic, mercury, selenium and antimony in environmental and biological samples based on hyphenated techniques. Molecules 24 (5), 926. https://doi.org/10.3390/molecules24050926

Zanin, L., Venuti, S., Zamboni, A., Varanini, Z., Tomasi, N., Pinton, R., 2017. Transcriptional and physiological analyses of Fe deficiency response in maize reveal the presence of strategy I components and Fe/P interactions. BMC Genomics 18, 154. https://doi.org/10.1186/s12864-016-3478-4

Zhang, J., Blackmer, A.M., Blackmer, T.M., 2009. Reliability of chlorophyll meter measurements prior to corn silking as affected by the leaf change problem. Commun. Soil Sci. Plant Anal. 40, 2087–2093. https://doi.org/10.1080/00103620902960609

Zhang, T., Zeng, X., Zhang, H., Lin, Q., Su, S., Wang, Y., Bai, L., Wu, C., 2019. The effect of the ferrihydrite dissolution/transformation process on mobility of arsenic in soils: investigated by coupling a two-step sequential extraction with the diffusive gradient in the thin films (DGT) technique. Geoderma 352, 22–32. https://doi.org/10.1016/j.geoderma.2019.05.042

Zhou, Z., Latta, D.E., Noor, N., Thompson, A., Borch, T., Scherer, M.M., 2018. Fe(II)-catalyzed transformation of organic matter-ferrihydrite coprecipitates: a closer look using Fe isotopes. Environ. Sci. Technol. 52, 11142–11150. https://doi.org/10.1021/acs.est.8b03407

Zhu, B., Jia, Y., Jin, Z., Sun, B., Luo, T., Kong, L., Liu, J., 2015. A facile precipitation synthesis of mesoporous 2-line ferrihydrite with good fluoride removal properties. RSC Adv. 5, 84389–84397. https://doi.org/10.1039/C5RA15619J

Zhu, J., Yang, X., Fan, F., Li, Y., 2018. Factors affecting the determination of iron species in the presence of ferric iron. Appl Water Sci 8 (8), 1–4. https://doi.org/10.1007/s13201-018-0876-6

Ferrihydrite Enrichment in the Rhizosphere of Unsaturated Soil Improves Nutrient Retention while Limiting Arsenic and Uranium Plant Uptake

Arindam Malakar,[1] Daniel D. Snow,[2] Michael Kaiser,[3] Jordan Shields,[4] Bijesh Maharjan,[5] Harkamal Walia,[3] Daran Rudnick,[6] and Chittaranjan Ray[7,*]

[1]Nebraska Water Center, part of the Robert B. Daugherty Water for Food Global Institute, Water Sciences Laboratory, University of Nebraska, Lincoln, Nebraska 68583-0844, United States.

[2]Nebraska Water Center, part of the Robert B. Daugherty Water for Food Global Institute, Water Sciences Laboratory and School of Natural Resources, University of Nebraska, Lincoln, Nebraska 68583-0844, United States.

[3]Department of Agronomy and Horticulture, University of Nebraska-Lincoln, Lincoln, Nebraska 68583-0915, United States.

[4]School of Natural Resources and Nebraska Water Center, part of the Robert B. Daugherty Water for Food Global Institute, Water Sciences Laboratory, University of Nebraska, Lincoln, Nebraska 68583-0844, United States.

[5]Department of Agronomy and Horticulture, University of Nebraska-Lincoln, Panhandle Research and Extension Center, 4502 AVE I Scottsbluff, Nebraska 69361-4939, United States.

[6]Biological Systems Engineering Department, 247 L.W. Chase Hall, University of Nebraska-Lincoln, Lincoln, Nebraska 68583-0726, United States.

[7]Nebraska Water Center, part of the Robert B. Daugherty Water for Food Global Institute 2021 Transformation Drive, University of Nebraska, Lincoln, Nebraska 68588-6204, United States.

*Corresponding Author: Chittaranjan Ray, Email: cray@nebraska.edu

Supplementary material

Tables S1 – S3

Figures S1 –S7

Supplementary material

Materials and Methods.

Porewater Analyses. Porewater samples were collected within 30 min after applying 1500 g of irrigation water and filtered using 0.45 μm syringe filter and sub-sampled. Porewater samples were analyzed spectrophotometrically (Vernier Spectrophotometer, USA) immediately after collection for reduced iron (Fe^{2+}) by 1,10-phenanthroline method, and for nitrite concentrations by coupling and diazotizing with sulfanilamide and N-(1-naphthyl)-ethylenediamine dihydrochloride at 510 nm and 538 nm, respectively (Kaifer, 1992; Oliveira et al., 2006; Tamura et al., 1974; Zhu et al., 2018). A subsample was preserved with hydrochloric acid for arsenic, uranium, and total iron quantification by inductively coupled plasma mass spectrometry (Thermo Dionex IC 5000+ iCAP RQ ICP MS) and for major cations (Na, K, Ca, Mg) using atomic absorption spectroscopy (Perkin Elmer AAnalyst 400 Spectrophotometer). Another subsample was acidified with sulfuric acid for colorimetric (Seal AQ2 Autoanalyzer) analyses of nitrate and ammonia. Unpreserved porewater samples were used for dissolved organic carbon (DOC) measurement by the persulfate oxidation method (Ol Model 1010 Carbon Analyzer), for major anion analysis in ion chromatography (Dionex ICS-90 Ion Chromatograph), alkalinity measurement by titrimetric method, and finally for arsenic speciation by ion chromatography (Dionex IonPac™ AS7 (2 mm i.d. by 250 mm length)) using ammonium carbonate as mobile phase followed by measurement in ICP-MS (Kutscher et al., 2012; Yu et al., 2019), within 24 hours of collection.

Soil and Plant Tissue Analyses. Soil field capacity was estimated after gravitational drainage. The pots (n=3) were filled with 8 kg of air-dried soil. The pots were saturated with water and allowed to drain gravimetrically until drainage stopped (48 hours), weighed, and field capacity was estimated. Soil pH was measured twice a week by 1:1 soil:water solution using a handheld

pH probe (Oakton PHTestrs 30). Soil water content was measured every other week and before porewater collection by oven drying at 105 ^{o}C for 24 hours. Soil oxidation-reduction potential (ORP) (Oakton ORPTestr 50) was measured biweekly at 5 cm depth, which utilized Ag/AgCl, KCl (Sat'd) as the reference electrode. ORP measurements were converted to Standard Hydrogen Electrode (SHE) using the Nernst equation and reported at E_h (V).

Acid-leachable arsenic and uranium quantification were carried out after microwave digestion of the air-dried soil samples (Link et al., 1998; United States Environmental Protection Agency (EPA), 1996). DCB extraction was carried out for quantifying extractable iron in the soil (Amaral et al., 2017; Malakar et al., 2020). All digests and extracts were analyzed without further dilution using ICP-MS and for iron after 100-fold dilution, with matrix match standards. Soil certified reference materials (CRMs) were processed using identical methods to check accuracy for elemental measurements.

The first group of plant samples (n=3) were harvested midpoint (Day 45) after 15 days of first porewater sampling. Crop samples were washed with reagent grade water and dried in an oven at 65 °C to constant weight. Plant dry biomass weight was recorded, roots and shoots were separated and analyzed separately in ICP-MS after microwave acid digestion. Similarly, at the endpoint (Day 105), the remaining crops (n=3) were harvested, dried, and biomass was recorded, separated to root, shoot, and grains/kernels. The dried samples were weighed and ground to pass through a 100-mesh sieve for elemental analysis with ICP-MS (United States Environmental Protection Agency (EPA), 1996).

Supplementary material

Table S1. Shows experimental arsenate concentration compared to aqueous speciation model predicted values in day 30, 60, and 90 for three Fh enriched systems.

Sampling Day	0.00% w/w Fh		0.05% w/w Fh		0.10% w/w Fh	
	Experiment	Model	Experiment	Model	Experiment	Model
	mol L^{-1}					
Day 30	$2.6*10^{-7}$	$2.3*10^{-7}$	$1.9*10^{-7}$	$2.2*10^{-7}$	$1.3*10^{-7}$	$1.6*10^{-7}$
Day 60	$6.1*10^{-7}$	$5.5*10^{-7}$	$5.2*10^{-7}$	$5.5*10^{-7}$	$1.8*10^{-7}$	$1.9*10^{-7}$
Day 90	$1.9*10^{-7}$	$1.7*10^{-7}$	$9.7*10^{-8}$	$1.0*10^{-7}$	$7.6*10^{-8}$	$7.7*10^{-8}$

Table S2. Shows experimental Fe^{2+} concentration compared to aqueous speciation model predicted values in day 30, 60, and 90 for three Fh enriched systems.

Sampling Day	0.00% w/w Fh		0.05% w/w Fh		0.10% w/w Fh	
	Experiment	Model	Experiment	Model	Experiment	Model
	mol L^{-1}					
Day 30	$2.1*10^{-6}$	$2.2*10^{-6}$	$2.0*10^{-6}$	$1.8*10^{-6}$	$1.5*10^{-6}$	$1.5*10^{-6}$
Day 60	$7.9*10^{-6}$	$8.1*10^{-6}$	$6.2*10^{-6}$	$6.1*10^{-6}$	$2.2*10^{-6}$	$2.1*10^{-6}$
Day 90	$4.8*10^{-7}$	$5.1*10^{-7}$	$9.3*10^{-7}$	$8.7*10^{-7}$	$8.6*10^{-7}$	$8.4*10^{-7}$

Table S3. Total soil arsenic and uranium concentration at the mid and endpoint of the experiment.

Fh Enrichment	Midpoint Arsenic	Endpoint Arsenic	Midpoint Uranium	Endpoint Uranium
	Mean±S.D. µg g^{-1}			
0.00% w/w Fh	2.24±0.10	2.85±0.24	1.10±0.04	1.44±0.30
0.05% w/w Fh	2.26±0.16	2.85±0.11	1.05±0.02	1.40±0.18
0.10% w/w Fh	2.28±0.41	2.82±0.43	1.17±0.20	1.49±0.36

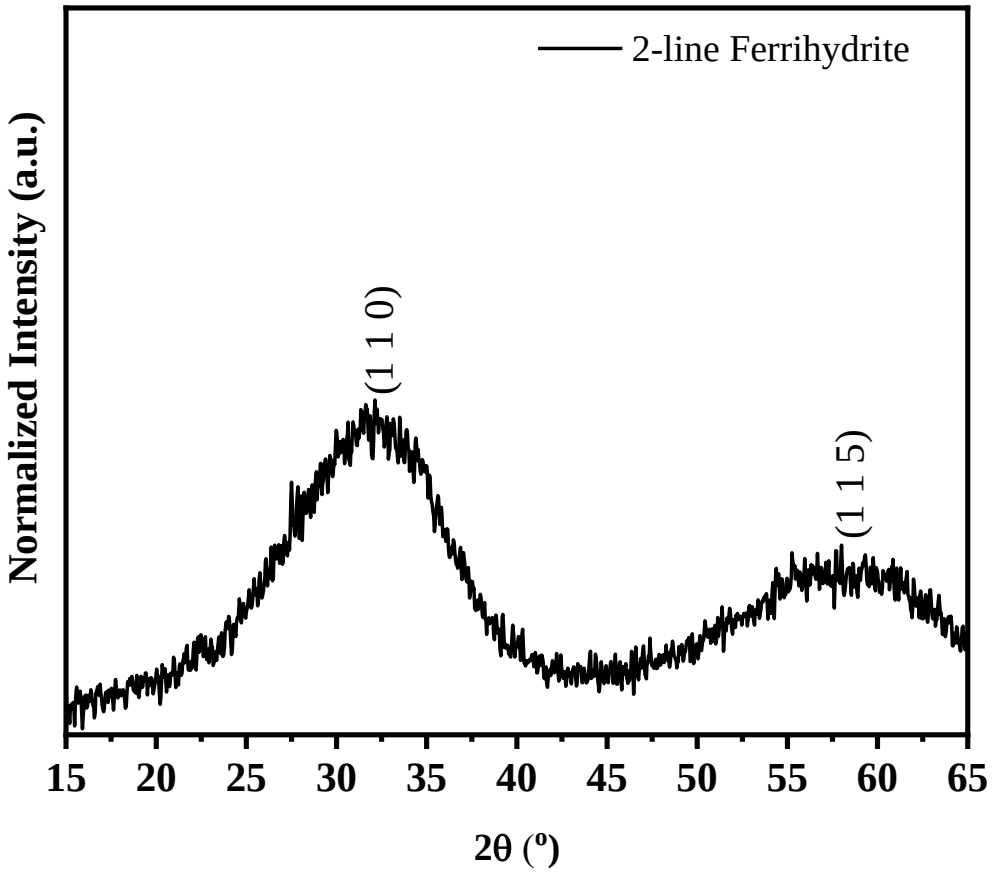

Figure S1. 2-line ferrihydrite powder x-ray diffraction data, matches well with PCPDF#29-0712 (Islam et al., 2020).

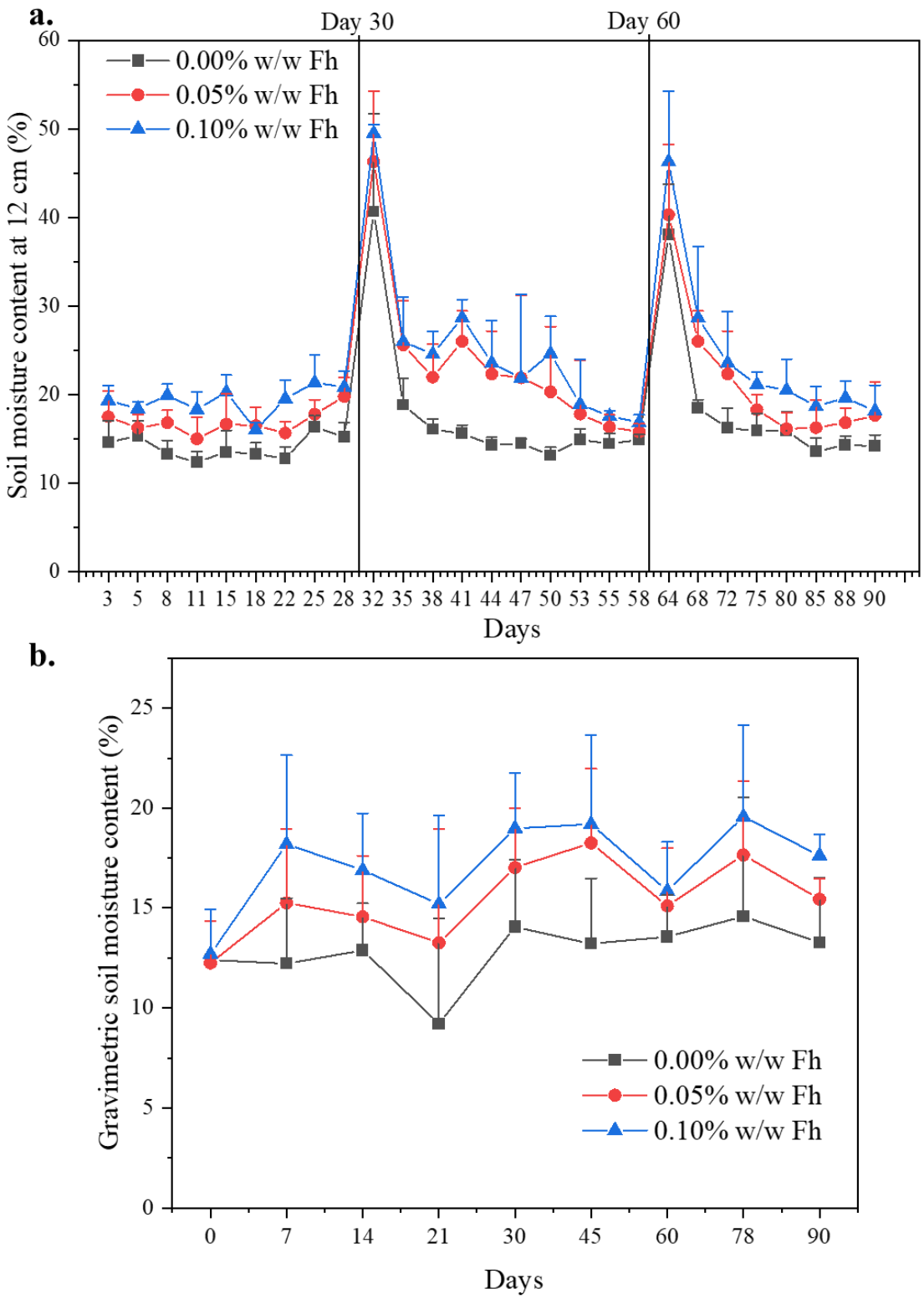

Figure S2. Soil moisture content **a.** at 15 cm depth measured by handheld moisture probe, **b.** gravimetric moisture content measured biweekly. Moisture profile of the handheld probe is very close to gravimetric moisture content and Fh enrichment seems to hold moisture better compared to control.

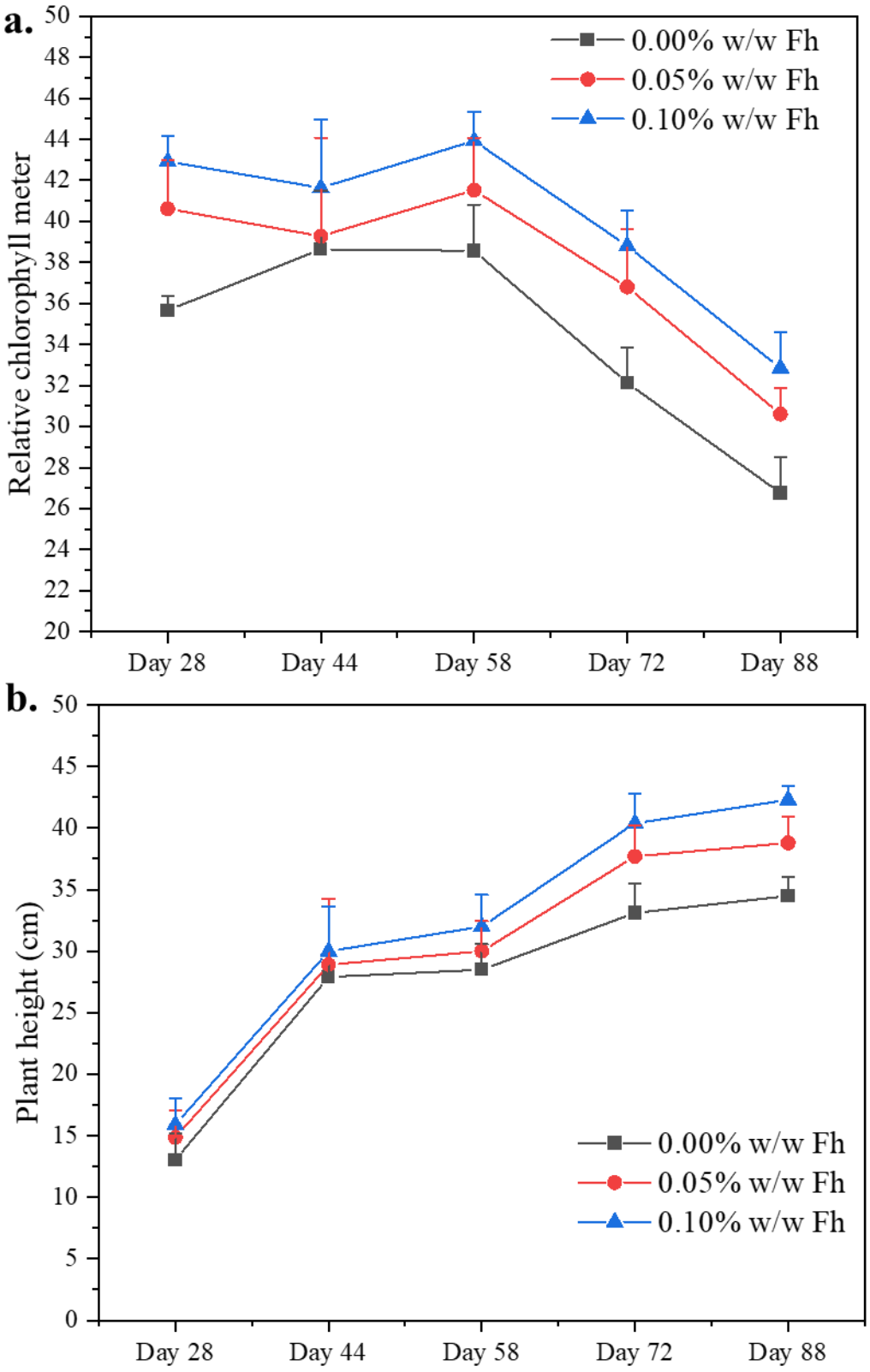

Figure S3. Shows (mean±standard deviation) **a.** relative chlorophyll content and **b.** plant height of crops grown under different Fh enriched soils.

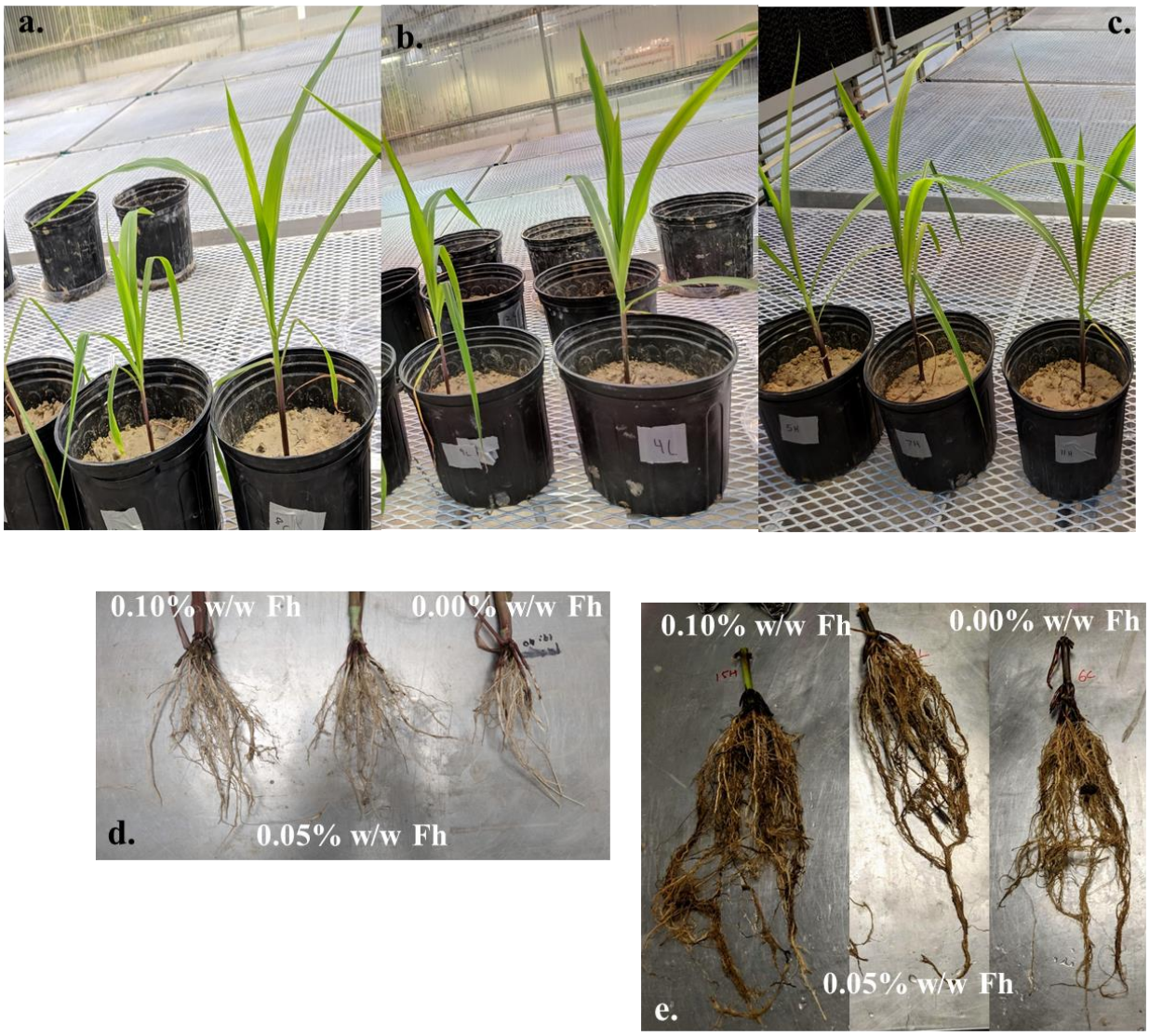

Figure S4. Shows corn in **a.** 0.00% w/w Fh, **b.** 0.05% w/w Fh, **c.** 0.10% w/w Fh enriched soil, **d.** roots of corresponding crops at day 45 and **e.** day 90.

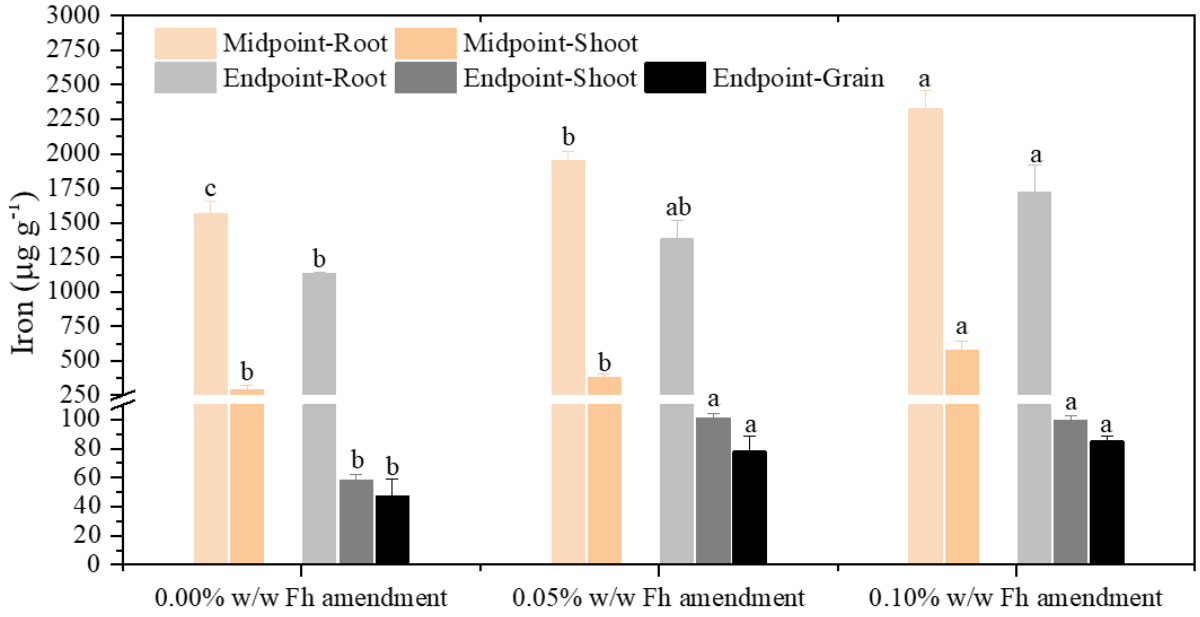

Figure S5. Shows concentration of iron in plant tissues – root, shoot at midpoint (day 45) harvest and root, shoot and grains at endpoint (day 90) harvest.

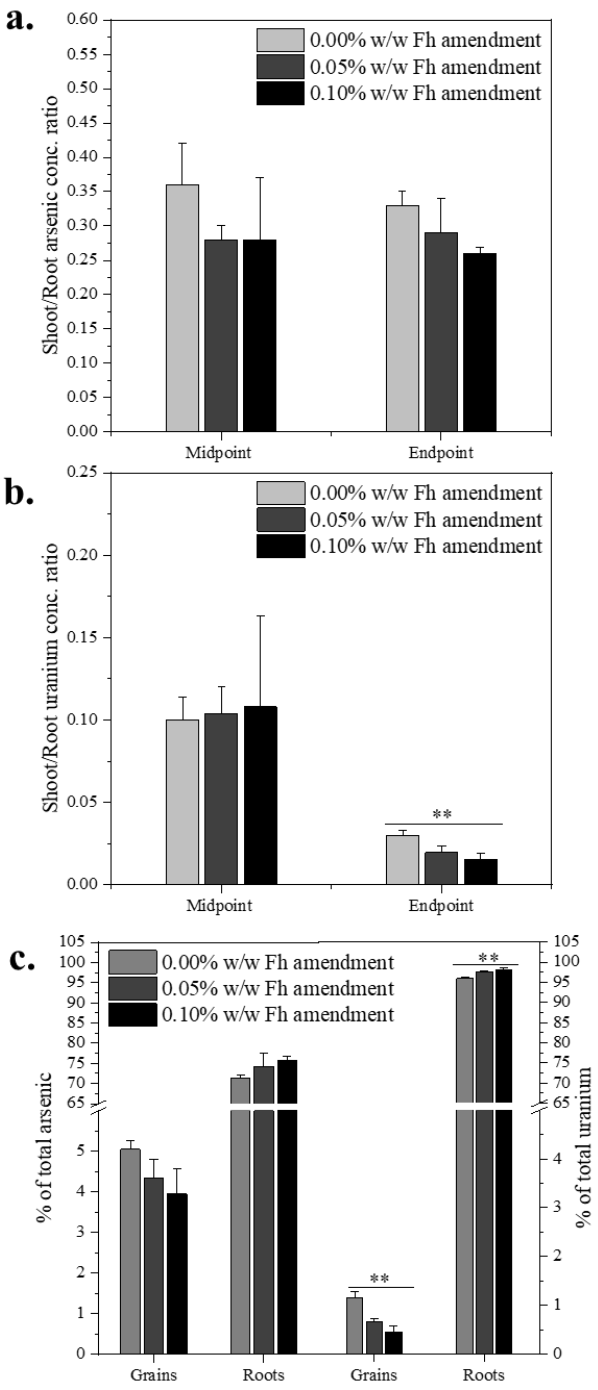

Figure S6. Shows **a.** Shoot to root arsenic, **b.** shoot to root uranium ratio and **c.** percentage (%) of total arsenic and uranium in grains and roots of crops at the endpoint of the experiment in three Fh enriched systems. Arsenic and uranium translocation within Fh enriched system is less compared to control.

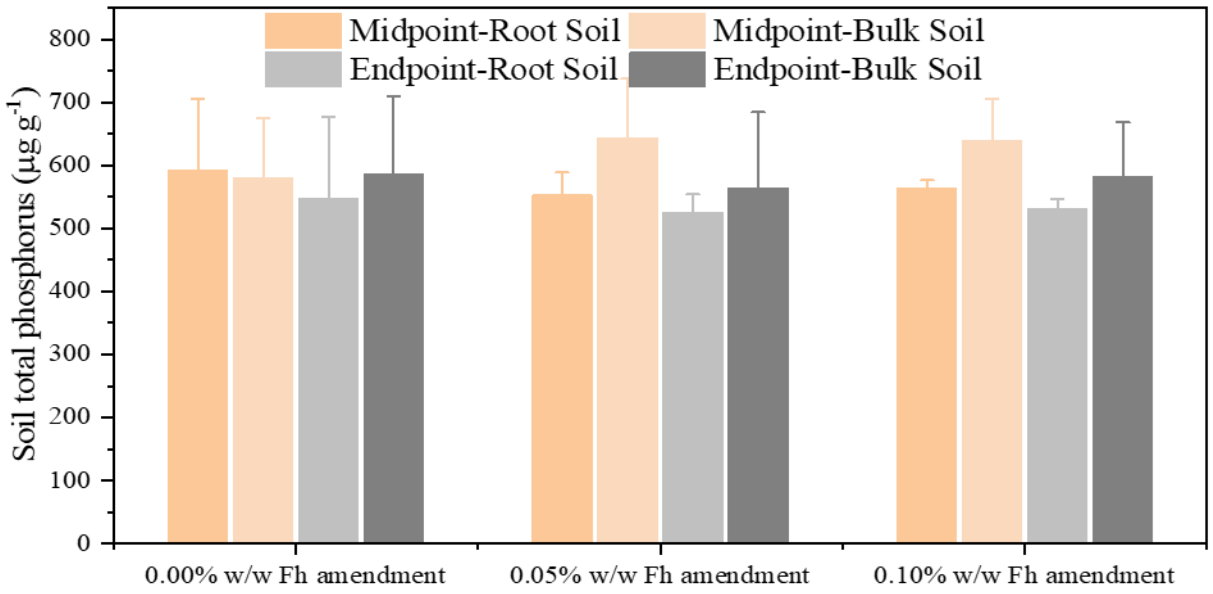

Figure S7. Total phosphorus concentration among the three different rates of Fh amendments at the root zone soil and bulk soil at mid (day 45) and endpoint (day 90) of the experiment.

References

Amaral, D.C., Lopes, G., Guilherme, L.R.G., Seyfferth, A.L., 2017. A New Approach to Sampling Intact Fe Plaque Reveals Si-Induced Changes in Fe Mineral Composition and Shoot As in Rice. Environ. Sci. Technol. 51, 38–45. https://doi.org/10.1021/acs.est.6b03558

Islam, S., Das, S., Mishra, G., Das, B., Malakar, A., Carlomagno, I., Meneghini, C., De Giudici, G., Gonçalves, L.P.L., Sousa, J.P.S., Kolen'ko, Y. V., Kuncser, A.C., Ray, S., 2020. Coagulating and flocculating ferrihydrite: application of zinc acetate salt. Environ. Sci. Water Res. Technol. 6, 2057–2064. https://doi.org/10.1039/D0EW00357C

Kaifer, A.E., 1992. Fundamentals of Analytical Chemistry. Sixth edition (Skoog, Douglas A.; West, Donald M.; Hollar, James F.), in: Journal of Chemical Education. p. A305. https://doi.org/10.1021/ed069pa305.1

Kutscher, D.J., McSheehy-Ducos, S., Wills, J., Jensen, D., 2012. IC-ICP-MS speciation analysis of As in apple juice using the Thermo Scientific iCAP Q ICP-MS (No. 43099).

Link, D.D., Walter, P.J., Kingston, H.M., 1998. Development and Validation of the New EPA Microwave-Assisted Leach Method 3051A. Environ. Sci. Technol. 32, 3628–3632. https://doi.org/10.1021/es980559n

Malakar, A., Kaiser, M., Snow, D.D., Walia, H., Panda, B., Ray, C., 2020. Ferrihydrite Reduction Increases Arsenic and Uranium Bioavailability in Unsaturated Soil. Environ. Sci. Technol. 54, 13839–13848. https://doi.org/10.1021/acs.est.0c02670

Oliveira, S.M., Lopes, T.I.M.S., Rangel, A.O.S.S., 2006. Spectrophotometric Determination of Nitrite and Nitrate in Cured Meat by Sequential Injection Analysis. J. Food Sci. 69, C690–C695. https://doi.org/10.1111/j.1365-2621.2004.tb09917.x

Tamura, H., Goto, K., Yotsuyanagi, T., Nagayama, M., 1974. Spectrophotometric determination of iron(II) with 1,10-phenanthroline in the presence of large amounts of iron(III). Talanta 21, 314–318. https://doi.org/10.1016/0039-9140(74)80012-3

United States Environmental Protection Agency (EPA), 1996. Method 3052: microwave assisted acid digestion of siliceous and organically based matrices.

Yu, X., Liu, C., Guo, Y., Deng, T., 2019. Speciation analysis of trace arsenic, mercury, selenium and antimony in environmental and biological samples based on hyphenated techniques. Molecules 24. https://doi.org/10.3390/molecules24050926

Zhu, J., Yang, X., Fan, F., Li, Y., 2018. Factors affecting the determination of iron species in the presence of ferric iron. Appl. Water Sci. 8. https://doi.org/10.1007/s13201-018-0876-6